Quaternary International 619 (2022) 12–29

Contents lists available at ScienceDirect

Quaternary International

journal homepage: www.elsevier.com/locate/quaint

Middle Pleistocene paleoclimate and paleoenvironment of central Italy and their relationship with hominin migrations and evolution

Alessandro Zanazzi [a,*], Andrew Fletcher [a,1], Carlo Peretto [b], Ursula Thun Hohenstein [b]

[a] Department of Earth Science, Utah Valley University, Orem, UT, USA
[b] Dipartimento di Studi Umanistici, Universita' degli Studi di Ferrara, Ferrara, Italy

ARTICLE INFO

Keywords:
Isernia La Pineta
Guado San Nicola
Stable isotope
Enamel
Stephanorhinus

ABSTRACT

To investigate the paleoclimate and paleoenvironment of central Italy during the Middle Pleistocene, we analyzed the carbon and oxygen stable isotope composition of the carbonate component of sequential enamel samples from twenty-four rhinoceros (*Stephanorhinus* spp.) teeth. The samples come from two key archeological and paleontological sites located in the Molise region: Isernia La Pineta (ILP; ~600 ka) and Guado San Nicola (GSN; ~400 ka).

Carbon isotope ratios of enamel from both ILP and GSN indicate feeding in a pure C_3 ecosystem that consisted predominantly of woodlands and/or mesic C_3 grasslands with the possible sparse presence of closed canopy forests at or near ILP ~600 ka. The average (± 1 σ) enamel $\delta^{13}C$ for ILP (−13.6 ± 0.6‰) is lower than that for GSN (−12.1 ± 0.4‰), suggesting higher mean annual precipitation and lesser aridity ~600 vs. ~400 ka. Average intra-tooth variability in enamel $\delta^{13}C$ from both sites is low (~1‰), likely indicating seasonally uniform diets, plant carbon isotope compositions, and precipitation amounts. However, the low intra-tooth variability in enamel $\delta^{13}C$ may also reflect amplitude attenuation of the isotopic signal of the plants into tooth enamel.

With respect to oxygen isotopes, the average (± 1 σ) enamel $\delta^{18}O$ for ILP (24.2 ± 0.7‰) is slightly lower than that for GSN (25.0 ± 0.7‰), likely reflecting the higher elevation of ILP as well as lesser aridity and/or slightly lower mean annual temperature in the region ~600 vs. ~400 ka. The $\delta^{18}O$ values of meteoric precipitation (~-7‰) calculated from enamel compositions are indistinguishable from the modern values, suggesting that mean annual temperatures were broadly similar to today (~13°C). Both sites exhibit a moderate average intra-tooth variability in enamel $\delta^{18}O$ (~2‰), likely indicating a temperature seasonality similar or slightly decreased relative to today. The temperate climate and the increase in aridity that occurred sometime between ~600 and ~400 ka were potentially important factors for the human colonization of the Italian peninsula and for the cultural and behavioral evolution of the early hominins during the Middle Pleistocene.

1. Introduction

The relationship between climate and human evolution is arguably one of the most studied and controversial research areas in paleoanthropology (e.g., see reviews in Bonnefille, 2010; Domínguez-Rodrigo, 2014; Kingston, 2007; Levin, 2015; Potts, 2013). More specifically, two topics have received considerable focus and have been the subject of numerous debates in the recent decades: the influence of climate and environment on the dispersals out of Africa and on the technological advances and adaptations of early hominins. For instance, some authors have suggested that early migrations and dispersals occurred in the context of grasslands or wooded grasslands similar to African savannas (Dennell and Roebroeks, 2005), while others have argued that migrating hominins tracked woodlands (Belmaker, 2010, 2011) or forests (Agustí and Lordkipanidze, 2019). Still others have suggested that instead of tracking or happening in the context of a specific habitat, migrating populations were driven by high climate variability (Potts and Faith, 2015). Finally, some studies ascribe the dispersals of early hominins to intrinsic morphological and behavioral factors such as the capacity for long distance walking and endurance running (Bramble and Lieberman, 2004; Steudel, 1994), heat adaptation (Walker et al., 1993), greater brain size (Aiello and Dunbar, 1993; Aiello and Wheeler, 1995), and

* Corresponding author.
E-mail address: alessandro.zanazzi@uvu.edu (A. Zanazzi).
[1] Present address: Conoco Philips, Houston, TX, USA.

https://doi.org/10.1016/j.quaint.2022.01.011
Received 4 June 2021; Received in revised form 17 January 2022; Accepted 18 January 2022
Available online 23 February 2022

social structure (Kroll, 1994), suggesting climate played a secondary role. With respect to cultural adaptations, recent studies performed in Africa suggested a primary role for aridification and the consequential variability of landscape resources in driving technological innovations (Owen et al., 2018; Patterson et al., 2017; Potts et al., 2020). In contrast, others found no connections between aridification and the ecological changes that have been widely thought to drive hominin evolution (Blumenthal et al., 2017). Potential support for the hypothesis linking aridification to technological innovations could come from investigations of climate records from archeological sites outside of Africa.

Given their strategic position between Africa and Eurasia, their well-dated sediments, the correspondence of their ages with those of critical paleoclimate and human evolution events, and their remarkable fossil records, Isernia La Pineta (ILP) and Guado San Nicola (GSN) are ideal sites to further investigate the influence of climate on human migrations and evolution in southern Europe. These two Middle Pleistocene open-air archeological and paleontological sites are located in the Italian region of Molise in the southern range of the Apennines (Fig. 1). Both sites have yielded abundant and well-preserved fossil fauna and artifacts indicating several periods of human occupations. The fossils and the artifacts are enclosed in clearly defined stratigraphic layers dominated by river and lake sediments interspersed with pyroclastic material (Channarayapatna et al., 2018; Coltorti et al., 1982, 2005; Peretto et al., 2004, 2015b). The Lower Paleolithic site of ILP, discovered in 1978, is located near the town of Isernia. $^{40}Ar/^{39}Ar$ dating of sanidine crystals yielded ages for the occupation layers of ~585 ka; this site therefore correlates with the end of Marine Isotope Stage (MIS) 15 (Peretto et al., 2015a). GSN, dating to the transition between the Lower and Middle Paleolithic, was discovered in 2005. It is located on the left bank of the Volturno River near the village of Monteroduni, ~10 km south of ILP. $^{40}Ar/^{39}Ar$ dating of sanidine crystals indicates the presence of humans between 400 and 365 ka; therefore this site correlates with the transition from MIS 11 to MIS 10 (Pereira et al., 2016). The main human activities conducted at the two sites were production of tools and butchering of animal carcasses for meat and marrow procurement (Alhaique et al., 2004; Peretto et al., 2015b). ILP and GSN are very important from both a paleoclimatology and human evolution perspective. In the context of paleoclimatology, the time period represented at ILP follows the transition from the 41-kyr to the 100-kyr glacial-interglacial cycles that occurred from the Early to the Middle Pleistocene, between 1.2 and ~0.6 Ma (Lisiecki and Raymo, 2005). The time represented at GSN, on the other hand, follows soon after the Mid-Brunhes Event (~430 ka), a global climate shift to markedly warmer interglacial conditions. In addition, MIS 11 (~410 ka) is considered the best analog for our present and future climate (see review in Candy et al., 2014). With respect to human evolution, ILP and GSN are characterized respectively by the presence of one of the oldest human fossils (Peretto et al., 2015a) and by the oldest evidence of prepared-core technologies (i.e., the Levallois method) in the Italian peninsula (Moncel et al., 2020; Pereira et al., 2016).

Previous paleoenvironmental and paleoclimatic studies conducted in the region are limited to faunal and palynological analyses. In terms of fossil fauna, the assemblage of ILP is characteristic of the Middle Galerian Mammal Age and representative of the Isernia Faunal Unit Biozone. The most well-represented taxon is *Bison schoetensacki*, followed by *Stephanorhinus hundsheimensis*, *Hippopotamus* cf. *antiquus*, *Premegaceros solilhacus*, *Cervus elaphus* cf. *acoronatus*, *Dama* cf. *roberti* (Breda et al., 2015), *Capreolous* sp., *Sus scrofa*, and *Hemitragus* cf. *bonali* (Sala, 1996). The remains of *Palaeoloxodon antiquus* are also present in large numbers (Breda et al., 2015). The most well-represented among the carnivores is the bear *Ursus deningeri*, but *Panthera leo fossilis* (Sala, 1996) and *Panthera pardus* (Sala, 2006) have also been reported. Additional taxa recovered from the upper sandy levels include *Hyaena* cf. *brunnea* (in layer 3s1-5), *Castor fiber*, and *Macaca sylvanus* (in layer 3s6-9) (Sala, 2006). The micromammal fauna has been attributed to the Early Toringian Small Mammal Age due to the presence of *Arvicola mosbachensis*, *Pliomys episcopalis*, *Microtus* (*Terricola*) *arvalidens*, and *Sorex* aff. *rutonensis* (Sala, 1983, 1996, 2006). *Talpa* sp., *Crocidura* sp., *Pliomys coronensis*, *Clethrionomys* sp., *Iberomys brecciensis* (López-García et al., 2015a; Sala, 1996), and *Microtus* gr. *arvalis-agrestis* are also present along with *Emys orbicularis*, *Anas platyhyncha*, and *Podiceps ruficollis* (Arobba et al., 2004; Sala, 1996; Tonon, 1988). This faunal assemblage suggests that the environment during the period of human occupation was dominated by an open steppe or grassland with scattered woody areas on the valley floor and along the rivers. Therefore, according to Sala (1996), the climate at ILP was generally dry with brief rainy periods during which the rivers occasionally flooded. The presence of *Macaca sylvanus* suggests the onset of a warmer interval during the time

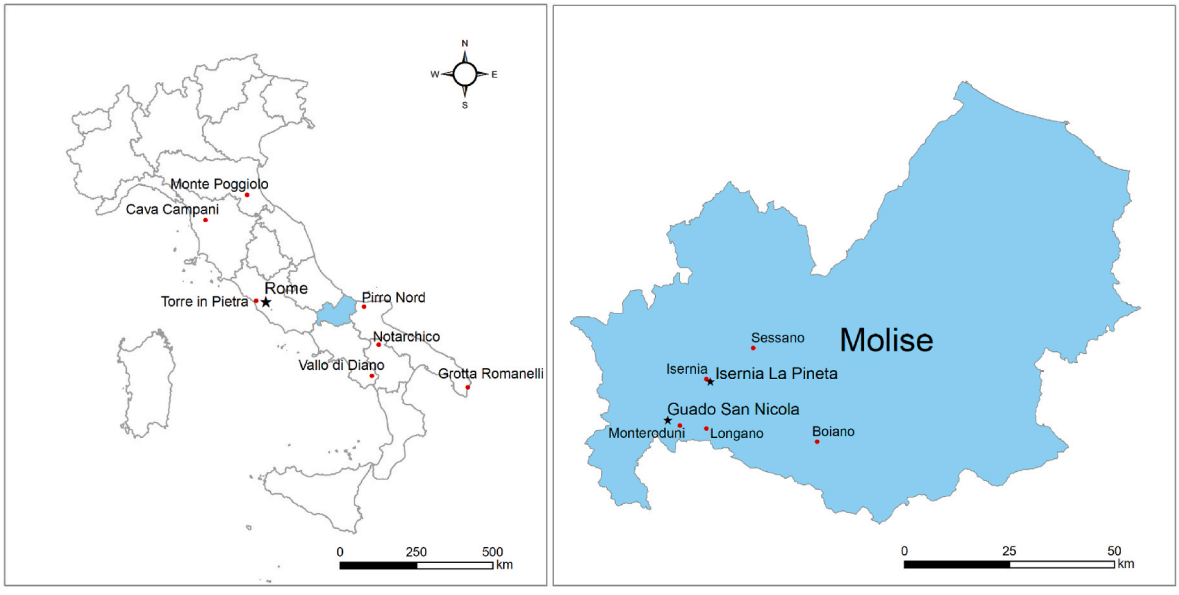

Fig. 1. Maps showing the location of the study sites and of all the Italian locations mentioned in the text. Left: map of Italy with Molise highlighted in blue. Right: map of Molise showing the location of the two study sites: Isernia La Pineta and Guado San Nicola.

represented by the upper sandy layers (3s6-9).

At GSN, the faunal assemblage includes species of both the Galerian and Aurelian mammal ages and can be associated with the Fontana Ranuccio Faunal Unit Biozone. The most well-represented taxon is *Equus ferus*, followed by *Palaeoloxodon* sp. and *Cervus elaphus acoronatus*. Cervidae, *Bos primigenius*, and *Stephanorhinus kirchbergensis* are also abundant whereas *Ursus* sp., Megacerini, and *Dama* sp. are represented only by a few samples. This faunal composition suggests a warm or temperate climate and the presence of woodland and shrub areas along with open grasslands (Peretto et al., 2015b).

With respect to pollen analysis, studies conducted at the Boiano and Sessano basins (located ~10 km from Isernia; Fig. 1) enabled the reconstruction of the flora from MIS 15 to MIS 9 (Amato et al., 2014; Ermolli et al., 2015; Orain et al., 2012, 2013a, 2013b). In general, during glacial periods, the environment was characterized by a steppe dominated by *Artemisia*, *Ephedra,* and Chenopodiacee with the minor presence of *Quercus*. During interglacial periods, the vegetation was dominated by mixed oaks along with *Pterocarya*, *Juglans*, and occasionally *Carya* (Orain et al., 2012, 2013a). Unfortunately, the richest archeological and paleontological units at ILP (Lebreton, 2002) and the entire sequence at GSN are sterile of pollen grains. Therefore, a complete reconstruction of the vegetation and paleoenvironment during the periods of human occupation is not possible by means of pollen analysis.

Given the importance of these two sites, the main goal of this study is therefore to further investigate the paleoclimate and paleoenvironment of ILP and GSN via carbon and oxygen stable isotope analysis of the carbonate component of fossil teeth from two species of rhinoceros, *Stephanorhinus hundsheimensis* and *Stephanorhinus kirchbergensis*. We selected rhinoceros because it is an abundant taxon at both sites and because its large body size and drinking behaviour likely allow its oxygen isotope composition to accurately record that of meteoric precipitation (Bryant and Froelich, 1995; Kohn, 1996; Kohn and Fremdt, 2007; Luz et al., 1984). In addition, tooth enamel was selected from among the biogenic mineralized tissues because it is the most resistant to diagenetic alteration and thefore it is more likely to preserve the original (i.e., biologic) isotopic signal (see review in Kohn and Cerling, 2002). Using anthropogenically-modified faunal remains such as *Stephanorhinus* spp. teeth from ILP and GSN has the advantage over almost all other climate proxies of providing a direct temporal link between the climate and the human occupation of the sites (Britton, 2017; Britton et al., 2019; Pederzani and Britton, 2019).

We utilized the isotopic data to answer the following specific questions:

1) What were the main dietary components of *Stephanorhinus* spp. and the main types of plants present at ILP and GSN ~600 and ~400 ka? We used the carbon isotope composition of rhinoceros tooth enamel to confirm the currently accepted view that after a peak abundance in the Middle Miocene, C_4 plants became rare or disappeared from southwestern Europe by the early Pliocene (Urban et al., 2016). In other words, we used isotopic data to confirm the expected dominance of C_3 plants in the diet of the rhinoceroses and in the ecosystems of ILP and GSN ~600 and ~400 ka.
2) What was the vegetation structure at ILP and GSN? What was the mean annual precipitation (MAP) at the two sites ~600 and ~400 ka? After confirming the presence of a pure C_3 ecosystem, we used the carbon isotope composition of rhinoceros tooth enamel to investigate the vegetation structure and ecosystem type at the two sites. We also calculated precipitation amounts by utilizing the global relationship between the carbon isotope composition of modern C_3 plants and MAP developed by Kohn (2010).
3) What was the oxygen isotope composition of meteoric precipitation at ILP and GSN ~600 and ~400 ka? We used the oxygen isotope composition of rhinoceros tooth enamel carbonate to estimate the composition of environmental (meteoric) waters. We then compared the compositions at the two sites with each other and with the modern value to speculate about changes in mean annual temperature (MAT) from ~600 to ~400 ka and from the Middle Pleistocene to the present.
4) What was the temperature and precipitation seasonality? Seasonal contrasts are even more important than annual averages in controlling the distribution of organisms. We therefore used the intra-tooth variability in the carbon and oxygen isotope composition of rhinoceros tooth enamel to qualitatively estimate the seasonal contrasts in temperature and precipitation.
5) How did the reconstructed climate and environment affect the migrations and evolution of early hominins in southern Europe? The answer to the previous questions allowed a better understanding of the paleoecological context in which early humans lived at these sites helping therefore to define a better framework for the conditions that affected the colonization of Europe and the adaptations developed by the early hominins during the Middle Pleistocene.

2. Background

2.1. Carbon isotope ratios in herbivore tooth enamel carbonate

Tooth enamel has a mineralogy similar to hydroxyapatite [$Ca_5(PO_4)_3(OH)$] with substitutions of the carbonate (CO_3^{2-}) for the phosphate (PO_4^{3-}) and hydroxyl (OH^-) ions (Driessens and Verbeeck, 1990). The carbon isotope composition of fossil tooth enamel carbonate from mammalian herbivores has been extensively used as a paleodietary and paleoenvironmental proxy. Studies have focused on both bulk samples for the reconstruction of the animals' average diet and habitat during the time of enamel formation and on intra-tooth sequential samples for the reconstructions of their seasonal variations (e.g., see reviews in Clementz, 2012; Fricke, 2010; Koch, 1998; Koch et al., 2007; Kohn and Cerling, 2002). Plants are the ultimate source of carbon for herbivores. Therefore, the main factor that affects the carbon isotope composition of herbivores' tooth enamel is the carbon isotope composition of the ingested plants (DeNiro and Epstein, 1978). In turn, the carbon isotope composition of plants is mainly determined by their photosynthetic pathway (Farquhar et al., 1989; O'Leary, 1988). Three different photosynthetic pathways have been identified: the C_3 (or Calvin Cycle), the C_4 (or Hatch-Slack), and the CAM (Crassulacean Acid Metabolism) pathways. CAM plants are mainly succulents (e.g., cacti); they represent a very minor fraction of terrestrial vegetation and for this reason they will not be considered further here. C_3 plants are trees, shrubs, cool-season grasses and sedges whereas C_4 plants are warm-season grasses and sedges (Farquhar et al., 1989; O'Leary, 1988). C_3 and C_4 plants have very distinctive carbon isotope compositions. All isotope compositions are expressed using the delta (δ) notation in parts per thousand or permil (‰) difference in relative abundance of the heavier isotope from that of a standard (V-PDB for $\delta^{13}C$ and V-SMOW for $\delta^{18}O$):

$$\delta = \frac{R_{sample}}{R_{standard}} - 1 \quad (1)$$

Where R is $^{13}C/^{12}C$ or $^{18}O/^{16}O$. The average $\delta^{13}C$ of modern C_3 and C_4 plants is ~-27‰ and ~-13‰, respectively (Ehleringer and Monson, 1993; Farquhar et al., 1989; Kohn, 2010; O'Leary, 1988). C_3 plants also show a larger range in $\delta^{13}C$ relative to C_4 plants (~14‰ vs. ~8‰). The reason for this larger range is that these plants can vary their discrimination against ^{13}C depending on local environmental conditions (e.g., light intensity, temperature, nutrient availability, and water stress) (Heaton, 1999). For instance, when water-stressed, these plants close their stomata and decrease their discrimination against ^{13}C. High $\delta^{13}C$ values are therefore characteristic of open, xeric C_3 grasslands (Farquhar et al., 1989). Conversely, very negative $\delta^{13}C$ values are found in humid closed canopy forests due to recycling of ^{13}C-depleted CO_2 and low irradiance (van der Merwe and Medina, 1991). The $\delta^{13}C$ of modern C_3 plants in the Mediterranean region shows a negative correlation with

both MAP and seasonal shifts in water availability (Hartman and Danin, 2010).

While the distinctive carbon isotope signature of the plants is captured by tooth enamel, biomineralization and metabolic processes result in the fractionation of carbon isotopes leading to an enrichment in ^{13}C in the carbonate component of herbivore enamel relative to plants that is mainly dependent on the digestive physiology of the animal (Cerling and Harris, 1999; Passey et al., 2005). This enrichment is reported in the literature as $\varepsilon_{enamel\text{-}plants}{}^{*}$, which is defined as follows:

$$\varepsilon^{*}_{enamel-plants} = \left(\alpha^{*}_{enamel-plants} - 1\right) \times 1000 \quad (2)$$

Where $\alpha_{enamel\text{-}plants}{}^{*}$ is the fractionation factor between enamel and the herbivore's diet:

$$\alpha^{*}_{enamel-plants} = \frac{\left(\frac{^{13}C}{^{12}C}\right)_{enamel}}{\left(\frac{^{13}C}{^{12}C}\right)_{plants}} \quad (3)$$

The $\delta^{13}C$ of the plants can be calculated from the $\delta^{13}C$ of the enamel and $\varepsilon_{enamel\text{-}plants}{}^{*}$ by applying the following equation:

$$\delta^{13}C_{plants} = \frac{1000 \times \left(\delta^{13}C_{enamel} - \varepsilon^{*}_{enamel-plants}\right)}{\varepsilon^{*}_{enamel-plants} + 1000} \quad (4)$$

Similarly, the $\delta^{13}C$ of the enamel can be calculated from the $\delta^{13}C$ of the plants and $\varepsilon_{enamel\text{-}plants}{}^{*}$ by applying the following equation:

$$\delta^{13}C_{enamel} = \frac{\delta^{13}C_{plants} \times \left(\varepsilon^{*}_{enamel-plants} + 1000\right) + \varepsilon^{*}_{enamel-plants} \times 1000}{1000} \quad (5)$$

For perissodactyls (odd-toed, non-ruminant or hindgut fermenter ungulates) including rhinoceroses, studies have shown that $\varepsilon_{enamel\text{-}plants}{}^{*}$ has mean values of 14.3 ± 1.6 to 14.7 ± 1.1‰ (Cerling and Harris, 1999; Harris et al., 2020; Passey et al., 2005). In this study, we therefore assume a value for this enrichment equal to 14.5‰. Calculating $\varepsilon_{enamel\text{-}plants}{}^{*}$ with the equation developed for all hindgut fermenters by Tejada-Lara et al. (2018) along with the average body mass inferred for *S. hundsheimensis* (~1350 kg) and *S. kirchbergensis* (~1800 kg) by Saarinen et al. (2016) produces a very similar value ($\varepsilon_{enamel\text{-}plants}{}^{*}$ = 14.2–14.3‰) and does not substantially change our conclusions. In addition, because the $\delta^{13}C$ of atmospheric CO_2 in the Middle Pleistocene was ~-7‰ (vs. a modern value of −8‰) (Tipple et al., 2010), a correction factor needs to be applied when reporting Pleistocene fossil ecosystems relative to a modern baseline or vice versa (Kohn and McKay, 2012; Kohn et al., 2005).

Based on enamel $\delta^{13}C$, the feeding environment of herbivores can be classified into closed canopy forests, woodlands-mesic C_3 grasslands, open woodlands-xeric C_3 grasslands, mixed C_3–C_4 grasslands, and pure C_4 grasslands (Domingo et al., 2013). The $\delta^{13}C$ of modern plants in closed canopy forests is lower than ~-30‰. Therefore, we applied equation (5) and the correction factor for the $\delta^{13}C$ of atmospheric CO_2 to calculate the cutoff in tooth enamel $\delta^{13}C$ that can be used to identify feeding in closed canopy forests by *Stephanorhinus* spp.:

$$\delta^{13}C_{enamel,\ closed\ canopy} < \frac{-30‰ \times (14.5 + 1000) + 14.5 \times 1000}{1000} + 1 \sim -14.9‰ \quad (6)$$

Similarly, the highest $\delta^{13}C$ of modern C_3 plants is ~-22‰ and the lowest $\delta^{13}C$ of modern C_4 plants is ~-17‰. As a result, the cutoffs in enamel $\delta^{13}C$ between open woodlands-xeric C_3 grasslands and mixed C_3–C_4 grasslands and between mixed C_3–C_4 grasslands and pure C_4 grasslands are ~-6.8% and ~-1.7%, respectively. Finally, the cutoff in enamel $\delta^{13}C$ between woodlands-mesic C_3 grasslands and open woodlands-xeric C_3 grasslands is the most difficult to define. Kohn et al. (2005) and Domingo et al. (2013) report a value for this cutoff of respectively −9‰ and −9.5‰ for Pleistocene ecosystems. Matson et al. (2012) compiled a list of plant $\delta^{13}C$ from modern ecosystems. Their lowest average $\delta^{13}C$ for xeric C_3 ecosystems is −24.8‰, which translates into a cutoff for enamel of ~-9.7‰, in good agreement with the estimates of Kohn et al. (2005) and Domingo et al. (2013).

In sum, *Stephanorhinus* spp. enamel $\delta^{13}C$ lower than −14.9‰ would indicate feeding in a closed canopy forest, between −14.9‰ and −9.7‰ would indicate feeding in a woodland-mesic C_3 grassland, and values between −9.7‰ and −6.8‰ would indicate feeding in an open woodland-xeric C_3 grassland. Finally, $\delta^{13}C$ values between −6.8‰ and −1.7‰ would indicate feeding in a mixed C_3–C_4 grassland and values higher than −1.7‰ would indicate feeding in a pure C_4 grassland. Based on the variability in the $\delta^{13}C$ of modern herbivores feeding in the same ecosystem (Drucker et al., 2008), we estimate an uncertainty for these cutoff values of ~± 1–2‰.

2.2. Oxygen isotope ratios in herbivore tooth enamel

The oxygen isotope composition of mammalian fossil tooth enamel has been widely used as a paleoclimate proxy for the reconstruction of both MAT's from bulk samples and temperature seasonality from intra-tooth sequential samples (e.g., see reviews in Clementz, 2012; Fricke, 2010; Koch, 1998; Koch et al., 2007; Kohn and Cerling, 2002; Pederzani and Britton, 2019). In principle, all three oxygen-bearing components of hydroxyapatite can be analyzed for their oxygen isotope compositions and the discussion below applies to the phosphate, carbonate, and hydroxyl components. However, most of the studies of fossil tooth enamel have focused on either the phosphate or carbonate component as the hydroxyl is readily altered by diagenetic processes (Kohn et al., 1999). The advantages of analyzing the phosphate are that it is thought to be more resistant to diagenesis (Zazzo et al., 2004) and that most of the early foundational work on the bioapatite paleothermometer was based on analyses of this component (e.g., Longinelli, 1984). In contrast, sample preparation for the analysis of the carbonate component is easier, results are more precise, and data on two isotopic systems (C and O) are obtained simultaneously.

With respect to oxygen isotopes, tooth enamel precipitates in equilibrium with body water (Bryant and Froelich, 1995). In turn, the $\delta^{18}O$ of body water is determined by the oxygen isotope composition of all oxygen inputs and outputs and their relative mass balance (Bryant and Froelich, 1995; Luz et al., 1984). In herbivorous mammals, the largest inputs are free water ingested with food, atmospheric oxygen, and drinking water (Kohn, 1996). Atmospheric oxygen has a globally constant $\delta^{18}O$ (Dole et al., 1954; Kroopnick and Craig, 1972) and therefore does not contribute to the variability in the $\delta^{18}O$ of body water. In contrast, drinking water and water ingested with food are typically either meteoric or meteoric-derived. At mid-latitudes, the isotopic composition of meteoric precipitation directly correlates with temperature, i.e., $\delta^{18}O$ values are higher when and where is warmer, lower when and where is colder (Rozanski et al., 1993). Hence, the oxygen isotope composition of tooth enamel from obligate drinkers can be used as a temperature proxy (e.g., see review in Koch, 1998). A few complications exist, however, when using enamel oxygen isotope ratios to reconstruct temperatures. Firstly, several additional factors affect the isotopic composition of mid-latitude meteoric precipitation (e.g., composition of the moisture source and air mass trajectories; Rozanski et al., 1993). Secondly, the correlation between the oxygen isotope composition of local meteoric water and that of teeth and bones is weak in non-obligate drinkers as these species obtain a larger proportion of their water from plants (Kohn and Cerling, 2002). Leaf-water is enriched in ^{18}O relative to surface water due to evapotranspiration (Flanagan et al., 1991). Evapotranspiration is low in dense humid forests where, as a result, obligate and non-obligate drinkers show similar enamel $\delta^{18}O$. However, the more arid the environment and the higher the evapotranspiration, the larger the difference will be between the enamel $\delta^{18}O$ of obligate and non-obligate drinkers (Levin et al., 2006). Modern

perissodactyls are, in general, obligate drinkers. Previous studies showed that the $\delta^{18}O$ of enamel from modern rhinoceroses shows a strong correlation with that of local meteoric water (Levin et al., 2006) and that ~80% of rhinoceroses' ingested water comes from drinking water (Clauss et al., 2005; Martin et al., 2008). *Stephanorhinus* enamel $\delta^{18}O$ therefore represents one of the best available proxies for the reconstruction of the composition of meteoric precipitation at ILP and GSN ~600 and ~400 ka.

2.3. Rhinoceros ecology

Studies on the cranial, post-cranial, and dental features of *S. hundsheimensis* and *S. kirchbergensis* indicate that they were medium to large-sized, two-horned rhinoceroses having slender, long limbs of cursorial proportions. Both species had brachydont dentition, with *S. kirchbergensis* being less brachydont than *S. hundsheimensis* (Ballatore and Breda, 2013; van Asperen and Kahlke, 2015). Based on their cranial and dental features, Mazza and Azzaroli (1993) concluded that European Pleistocene rhinoceroses recalled extant African species more than the Asian ones. In addition, these authors inferred that *S. hundsheimensis* likely had a strong prehensile upper lip and bore his head uplifted, suggesting that its diet and habitat were similar to those of the "black" or "hooked-lipped" rhinoceros *Diceros bicornis*. This extant species is a browser living in central and southern Africa in open scrub woodlands and marginal small woods and feeding on leaves, shrubs, twigs, and occasionally fruits (Macdonald, 2007). Mazza and Azzaroli (1993) also inferred that *S. kirchbergensis* likely bore his head drooping and lacked a prehensile upper lip, being therefore probably a "square-lipped" rhinoceros similar to *Ceratotherium simum*. This extant species (commonly referred to as the "white rhinoceros") is a grazer inhabiting open grasslands in southern and northeastern Africa (Macdonald, 2007).

Results from mesowear studies conducted on these Pleistocene rhinoceroses are apparently in conflict with each other and with those from the morphological studies described above. For instance, Hernesniemi et al. (2011) compared mesowear scores for the extant rhinoceroses with scores for four Pleistocene species from the UK. Cluster analysis of these data grouped *S. kirchbergensis* with the Sumatran rhinoceros (*Dicerorhinus sumatrensis*) and *S. hundsheimensis* with the Javan rhinoceros (*Rhinoceros sondaicus*). Both of these extant species are browsers living in dense rain forests (Macdonald, 2007). In contrast with these results, van Asperen and Kahlke (2015) obtained mesowear data for *S. hundsheimensis* and *S. kirchbergensis* from Germany and the UK. They concluded that in comparison with the extant Asian and African rhinoceroses, most European Middle Pleistocene *Stephanorhinus* spp. individuals had a diet that was shifted more towards the mixed feeder-grazer end of the dietary spectrum. According to these authors, extant rhinoceroses do not provide suitable dietary analogs for European Pleistocene rhinoceroses. All of their analyzed *S. kirchbergensis* populations were classified as mixed feeders. One of their *S. hundsheimensis* population was classified as a mixed feeder and another as a browser. Finally, Kahlke and Kaiser (2011) analyzed mesower data for two populations of *S. hundsheimensis* from two different locations in Germany. Based on their data, one population was classified as grazers having the reedbuck antelope (*Redunca redunca*) as the best modern analog. Among the extant rhinoceroses, *C. simum* is likely most similar to this ancient population. In contrast, the second population was classified as browsers most similar to *D. sumatrensis*. The authors' conclusion was that *S. hundsheimensis* had the most pronounced dietary variability ever recorded for a single herbivorous ungulate species. Overall, these mesowear studies seem to indicate that while *S. kirchbergensis* was more specialized than *S. hundsheimensis*, both retained a considerable dietary flexibility and adapted their diet according to the avaliability of food resources in different habitats (van Asperen and Kahlke, 2015).

3. Material and methods

3.1. Study sites

ILP (41.5922° N; 14.2406° E) is located near the town of Isernia on the left bank of the Cavaliere Stream at an elevation of 451 m (Fig. 1). The town currently has a MAT of ~13°C (Brunetti et al., 2014), a MAP of 958 mm/yr, and a mean annual range of temperature (MART) of ~18°C (Desiato et al., 2015). Maximum (141 mm) and minimum (39 mm) precipitation occur in November and July, respectively (Desiato et al., 2015). The site belongs to the "Le Piane Basins" fluvio-lacustrine sedimentary sequence which contains volcanic components mainly associated with the eruptions of Roccamonfina volcanoes. The infilling of the basins is characterized by four major unconformity-bounded stratigraphic units that lie on a bedrock composed of Tertiary limestone. These units were deposited from the Early Pleistocene to the Holocene (Brancaccio et al., 1997, 2000). The archeological layers have been identified within five stratigraphic units interspersed with paleosols. From the bottom, these units are (Fig. 2): 1) U5, composed of lacustrine muds; 2) U4, composed of calcareous tufa with pyroclastic sediments in the upper part; 3) U3, which is subdivided in three subunits (U3A, U3E, U3F), includes sands rich in volcanic materials and thin layers of gravels deposited by ephemeral streams; 4) U2, composed of gravels with thin sand layers deposited by seasonal streams with the upper part corresponding to a deeply altered paleosol; and 5) U1, corresponding to a sequence of colluviums with the presence of paleosols in the upper part (Coltorti et al., 1982, 2005). The archeological layers are located in the upper part of U4 (3c) and in the subunit U3E (3a and 3s10); the teeth analyzed in this study are from layers 3coll, 3s10, 3s6-9, 3s1-5 (all in U3E; Fig. 2). The eruption $^{40}Ar/^{39}Ar$ age of pumice found in U4 is 585 ± 1 ka. In addition, sanidine crystals reworked from the pumice and found in layers 3coll, 3s10, and 3s6-9 yielded minimum depositional $^{40}Ar/^{39}Ar$ ages of 586 ± 2 ka, 583 ± 3 ka, and 587 ± 2 ka, respectively (Peretto et al., 2015a).

GSN (41.5306° N; 14.1500° E) is located in the Sant'Eusanio district of the village of Monteroduni at an elevation of 247 m (Fig. 1). The village currently has a MAP of 1038 mm/yr. Similar to Isernia, maximum (170 mm) precipitation occurs in November while minimum (34 mm) precipitation occurs in July (Desiato et al., 2011). The site is situated on the left bank and within the oldest Middle Pleistocene terrace of the Volturno River in an ancient alluvial fan of the Lorda River, a tributary of the Volturno. Its stratigraphic sequence shows coarse sediments mainly deposited by braided streams and finer sediments mainly deposited by meandering streams (Peretto et al., 2015b). The whole fluvial sequence is rich in pyroclastic material. Like the volcanic material found at ILP, the source of the pyroclasts were the Roccamonfina volcanoes (Pereira et al., 2016). Briefly, the following stratigraphic units are distinguished from the bottom to the top in the excavation area (Fig. 3): 1) S.U. E, composed of fluvial gravel and sand; 2) S.U. D, composed of fluvial silt, sand, and clay; 3) S.U. C, composed of fluvial silt and sand with abundant pumice; 4) S.U. B*C, composed of gravel deposited by a debris flow; 5) S.U. B, in erosive contact with S.U. C and S.U. B*C and composed of sand and gravel with some volcanic material and deposited by two debris flows; 6) S.U. A*B, composed of pedogenically modified darker gravelly silty sand deposited by another debris flow; 7) S.U. A, composed of sand deposited by an earth flow and rich in pumice. Near the excavation area, three additional units can be identified: 1) S.U. Tufi, a tephra layer deposited directly in the Lorda

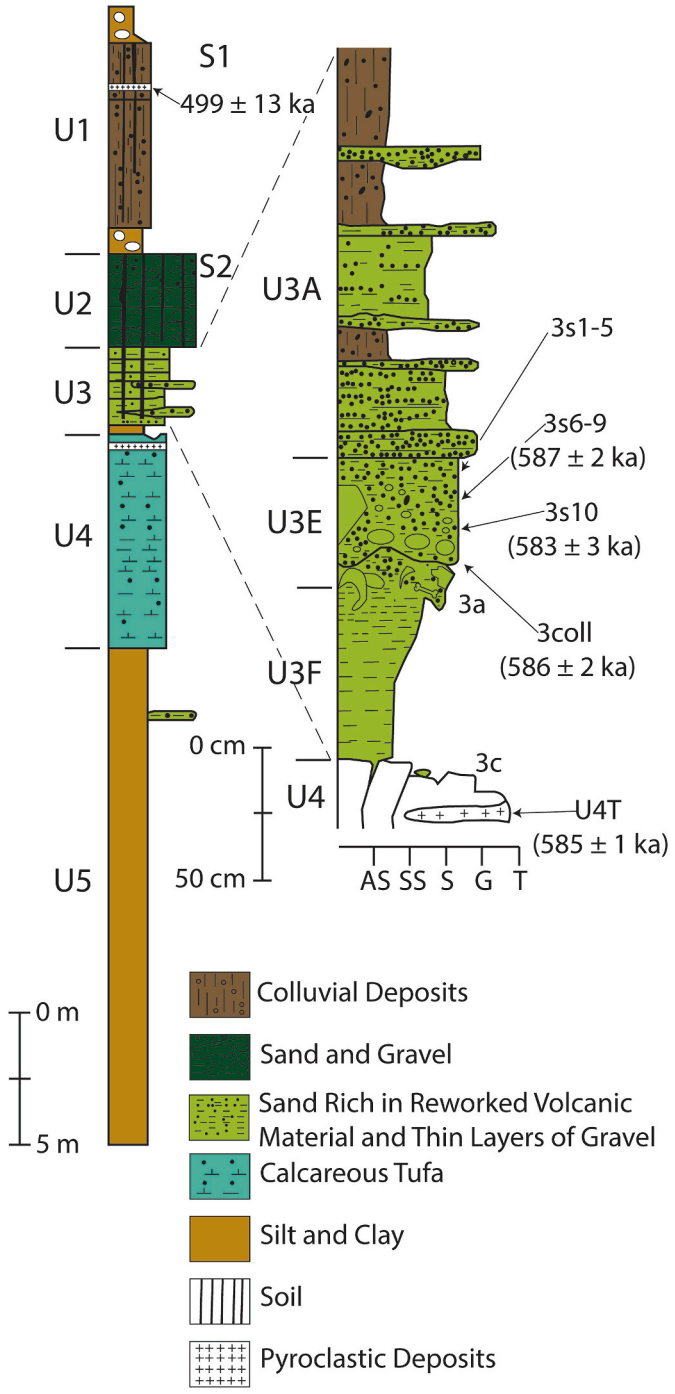

Fig. 2. Stratigraphy of Isernia La Pineta (modified from Peretto et al., 2015a), which is characterized by 5 main units (U1 to U5) and 2 buried paleosols (S1 and S2). The details of the stratigraphy of U3 is shown on the right. This unit contains various sedimentological layers (U3A, U3E, U3F), including two major archeological layers (3a and 3c). $^{40}Ar/^{39}Ar$ dates are from Peretto et al. (2015a). The analyzed teeth come from 4 layers (3coll, 3s10, 3s6-9, and 3s1-5) in U3E. AS: silts and clays; SS: silts and fine sands; S: medium to coarse sands; G: gravels; T: calcareous tufa.

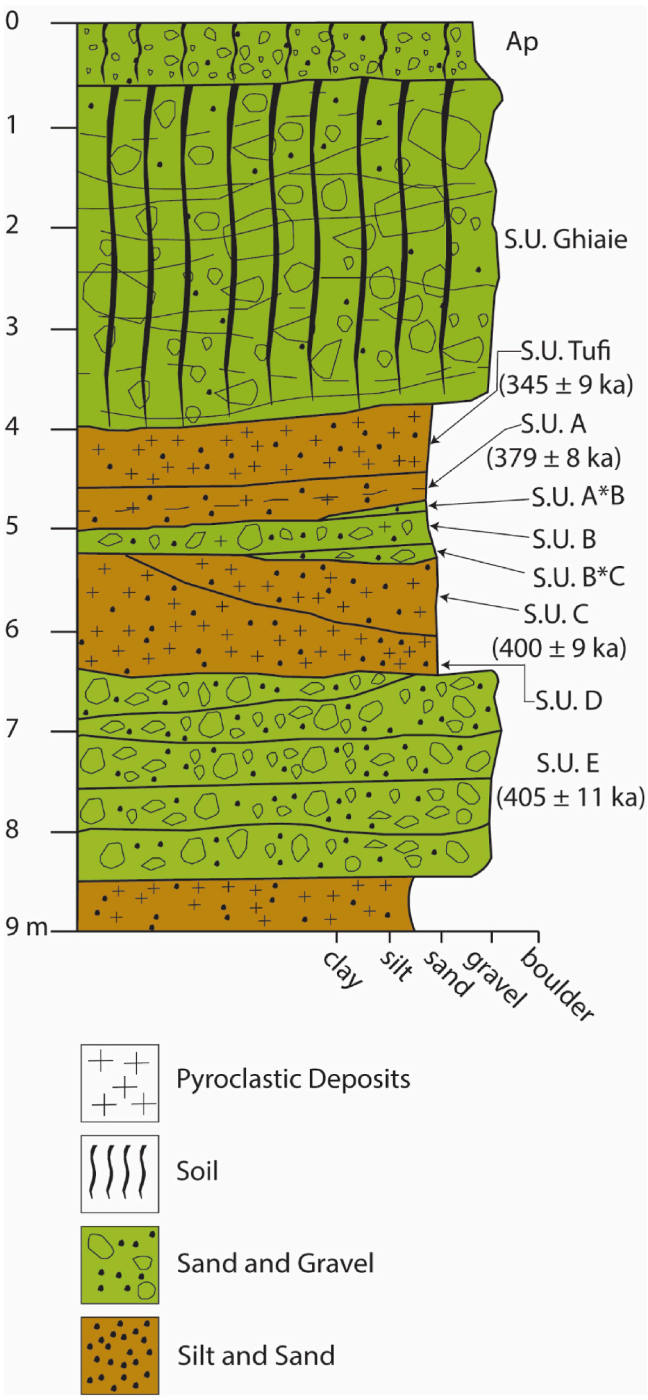

Fig. 3. Stratigraphy of Guado San Nicola (modified from Peretto et al., 2015b), showing the seven units found in the excavation area (S.U. E, S.U. D, S.U. C, S.U. B*C, S.U. B, S.U. A*B, and S.U. A) as well as the three units found nearby (S.U. Tufi, S.U. Ghiaie, and Ap). $^{40}Ar/^{39}Ar$ dates are from Pereira et al. (2016). The analyzed teeth come from S.U. C, S.U. B*C, S.U. B, and S.U. A*B.

River; 2) S.U. Ghiaie, composed by coarse gravel; 3) Ap, paleosol (Argillisol) characterized by a succession of decarbonated and argillic horizons. The teeth analyzed in this study are from S.U. C, S.U. B*C, S.U. B, and S.U. A*B, which are the only units rich in lithic tools and faunal remains. Sanidine crystals from the primary volcanic deposits of S.U. E and S.U. Tufi yielded eruption $^{40}Ar/^{39}Ar$ ages of 405 ± 11 ka and 345 ± 9 ka, respectively. In addition, sanidine crystals (likely reworked) from S.U. C and S.U. A yielded minimum depositional $^{40}Ar/^{39}Ar$ ages of 400 ± 9 ka and 379 ± 8 ka, respectively. Finally, 6 teeth from S.U. B*C and S.U. C yielded a mean ESR/U-series age of 364 ± 36 ka. The four archeological layers therefore span an interval from 400 ± 9 ka to 345 ± 9 ka (Pereira et al., 2016).

Table 1
Summary statistics of the $\delta^{13}C$ and $\delta^{18}O$ values of the *Stephanorhinus* teeth analyzed in this study.

Site	UVU Sample ID	Stratigraphic Layer	Taxon	Tooth Position	n subsamples	$\delta^{13}C$ Average (‰)	$\delta^{13}C$ Range (‰)	$\delta^{13}C$ SD (‰)	$\delta^{18}O$ Average (‰)	$\delta^{18}O$ Range (‰)	$\delta^{18}O$ SD (‰)
Isernia La Pineta	Q134	3 coll	*S. hundsheimensis*	Upper cheek tooth	26	−13.2	1.2	0.3	23.7	1.4	0.4
Isernia La Pineta	Q126	3 coll	*S. hundsheimensis*	Upper cheek tooth	5	−13.0	0.7	0.3	22.7	0.8	0.3
Isernia La Pineta	Q99	3 coll	*S. hundsheimensis*	Cheek tooth	21	−13.8	0.6	0.2	24.2	1.4	0.4
Isernia La Pineta	Q114	3 coll	*S. hundsheimensis*	Upper cheek tooth	8	−13.0	0.2	0.1	23.2	1.5	0.5
Isernia La Pineta	Q105	3 coll	*S. hundsheimensis*	Upper cheek tooth	8	−12.9	0.4	0.1	24.2	1.1	0.4
Isernia La Pineta	Q70	3 coll	*S. hundsheimensis*	Upper left M1	11	−13.3	0.7	0.2	23.6	1.2	0.4
Isernia La Pineta	Q69	3 coll	*S. hundsheimensis*	Upper right M2	21	−14.6	1.2	0.3	24.6	3.1	0.7
Isernia La Pineta	Q135	3s10	*S. hundsheimensis*	Upper cheek tooth	12	−14.0	0.9	0.3	25.2	1.8	0.6
Isernia La Pineta	Q95	3s6-9	*S. hundsheimensis*	Upper cheek tooth	20	−14.3	0.6	0.2	24.9	1.5	0.4
Isernia La Pineta	Q148	3s6-9	*S. hundsheimensis*	Premolar	17	−13.4	1.3	0.2	24.4	1.7	0.6
Isernia La Pineta	Q106	3s6-9	*S. hundsheimensis*	Upper cheek tooth	12	−14.1	0.6	0.2	25.1	1.3	0.4
Isernia La Pineta	Q175_21	3s1-5	*S. hundsheimensis*	Upper cheek tooth	7	−13.6	0.3	0.1	24.3	0.7	0.3
Isernia La Pineta	Q135	3s1-5	*S. hundsheimensis*	Upper cheek tooth	14	−13.9	0.6	0.1	24.0	0.9	0.3
Isernia La Pineta	Q175_7	3s1-5	*S. hundsheimensis*	Lower cheek tooth	7	−13.8	0.6	0.2	23.9	0.9	0.3
Isernia La Pineta	Q194	3s1-5	*S. hundsheimensis*	Cheek tooth	8	−13.5	0.9	0.3	23.8	1.4	0.5
Isernia La Pineta	Q104	3s1-5	*S. hundsheimensis*	Cheek tooth	23	−13.1	1.3	0.4	24.1	1.8	0.5
Isernia La Pineta	Q165	3s1-5	*S. hundsheimensis*	Upper right M3	11	−13.8	0.6	0.2	23.7	0.9	0.3
Guado San Nicola	QO13	S.U. C	*S. kirchbergensis*	Lower right cheek tooth	26	−12.0	0.9	0.2	25.0	1.7	0.5
Guado San Nicola	QP10	S.U. B*C	*S. kirchbergensis*	?	9	−13.2	1.1	0.3	25.3	1.1	0.3
Guado San Nicola	QQ12	S.U. B*C	*S. kirchbergensis*	Lower tooth	8	−11.8	0.4	0.1	23.9	1.8	0.6
Guado San Nicola	QN13	S.U. B	*S. kirchbergensis*	Lower tooth	19	−12.4	0.9	0.2	25.0	2.4	0.6
Guado San Nicola	QS11	S.U. B	*S. kirchbergensis*	?	21	−11.8	0.7	0.2	25.2	1.9	0.4
Guado San Nicola	QQ9	S.U. A*B	*S. kirchbergensis*	Upper left P4	11	−12.0	0.8	0.2	25.0	1.9	0.6
Guado San Nicola	QP9	S.U. A*B	*S. kirchbergensis*	Right P1	13	−12.1	0.9	0.2	25.0	1.1	0.3

3.2. Tooth samples

Rhinoceros remains at both ILP and GSN are represented for the most part by isolated teeth and other cranial elements followed by vertebrae, phalanges, and limb bones showing butchering traces related to the intentional fracturing of the long bones to recover the marrow (Giusberti and Peretto, 1991; Thun Hohenstein et al., 2002). Among all the teeth of the collection, we selected 24 well-preserved ones to analyze for this study: 17 from ILP (7 from 3coll, 1 from 3s10, 3 from 3s6-9, and 6 from 3s1-5) and 7 from GSN (1 from S.U. C, 2 from S.U. B*C, 2 from S.U. B, and 2 from S.U. A*B). Most of the selected teeth are complete molars and premolars (Table 1). Cheek teeth of *Stephanorhinus* are morphologically very similar (Ballatore and Breda, 2013); the identification of the exact position in the tooth row was therefore in most cases not possible. Eruption order of permanent teeth in extant rhinoceroses is usually M1-M2-P2-P3-P4-M3 (Groves, 1967; Guérin, 1980), however the timing of eruption of the M2 is irregular and can occur after the P2 and before the P3 (Tong, 2001). As enamel formation of the M1 and M2 starts during intra-uterine life (Martin et al., 2008), the isotopic composition of a few of our investigated teeth may have been affected by nursing because milk has higher $\delta^{18}O$ than drinking water and lower $\delta^{13}C$ than plants. The higher $\delta^{18}O$ in the mother's body water and milk relative to drinking water is the result of the preferential loss of ^{16}O through expired and transcutaneous water vapor fluxes (Kohn et al., 1996). The

lower $\delta^{13}C$ in milk relative to plants is due to the presence of lipids, which are depleted in ^{13}C relative to other macronutrients (DeNiro and Epstein, 1977). However, the effect of nursing on the $\delta^{13}C$ of our investigated teeth is likely to be very small as rhinoceroses' milk has very low lipid content (Osthoff et al., 2021). A slightly bigger effect on $\delta^{18}O$ is possible, but several studies showed no clear pattern in the $\delta^{18}O$ of the M1's relative to the other teeth (Ecker et al., 2013; Gadbury et al., 2000; Luyt and Sealy, 2018; Murphy et al., 2007; Zazzo et al., 2002). All of the teeth were isolated, therefore it was not possible to determine the number of rhinoceros individuals represented in our sample set. The teeth from ILP belong to *Stephanorhinus hundsheimensis* (the so-called Hundsheim rhinoceros), a medium-sized rhinoceros very common in European late Early to Middle Pleistocene assemblages (Fortelius et al., 1993; Lacombat, 2005; Mazza et al., 1993; Schreiber, 2005; van der Made, 2010). This rhinoceros appeared in Europe between 1.4 and 1.2 Ma and survived until 0.6–0.5 Ma (Kahlke and Kaiser, 2011). The teeth from GSN belong to the larger and more specialized *Stephanorhinus kirchbergensis* (the so-called forest or Merck's rhinoceros). After a period of sympatry between 0.7 and 0.6 Ma, *S. kirchbergensis* replaced *S. hundsheimensis* in temperate European faunas and survived until MIS 4–3 (Lacombat, 2005, 2006).

3.3. Tooth enamel mineralization and sampling stategy

The formation of mammalian dental enamel involves two phases (Balasse, 2002; Hoppe et al., 2004b; Passey and Cerling, 2002; Tafforeau et al., 2007; Trayler and Kohn, 2017). In a first phase (called apposition), a partially mineralized organic matrix is secreted by specialized cells called ameloblasts. Apposition contributes 25% wt of the total phosphate and 50% wt of the total carbonate of enamel. In the second phase (called maturation), the appositional organic matrix is progressively removed along with pore fluids, enamel mineralization increases as crystals widen and thicken, and the remaining 75% wt of phosphate and 50% wt of carbonate are deposited to produce a final hydroxyapatite concentration of ~95% wt in enamel (Trayler and Kohn, 2017). Both phases proceed from the occlusal surface to the root but not at the same rate and geometry. The appositional front proceeds at low angle relative to the enamel-dentine junction (EDJ) (Hoppe et al., 2004b; Trayler and Kohn, 2017). In contrast, the geometry of maturation can be complex, but the front seems to proceed in most cases at high angles relative to the EDJ (Green et al., 2017; Passey and Cerling, 2002; Trayler and Kohn, 2017). In addition, maturation is faster and occurs earlier in the inner and central enamel layers than in the outer layer (Trayler and Kohn, 2017). Mineralization becomes eventually highest in a narrow subsurface layer (Suga, 1982) while carbonate content decreases by ~2% wt (from ~5% wt to ~3% wt) from the EDJ to the outer surface (Zazzo et al., 2005).

Enamel apposition produces different types of incremental features. Cross-striations are short straight lines perpendicular to enamel prisms that reflect the circadian activity of ameloblast activity. Retzius striae are lines that correspond to successive positions of the appositional front. Finally, laminations are daily, regularly spaced lines parallel to Retzius striae that are temporally equivalent to cross-striations (Tafforeau et al., 2007). The enamel enclosed by two Retzius striae is referred to as a Retzius band, and the time required to deposit a Retzius band is called periodicity. The periodicity is constant for different individuals of the same species and can be determined by counting the number of cross-striations per Retzius band. Once the periodicity is known, appositional crown formation times can be determined by counting the number of Retzius bands in a crown. Tafforeau et al. (2007) estimated appositional crown formation times of ~2–4 years for rhinoceroses' molars.

The complexity of enamel mineralization poses challenges in the sequential sampling of enamel for the reconstructions of seasonal climatic and environmental changes. Maturation can take weeks to months and in some parts of the enamel there can be a substantial time lag between apposition and maturation (Hoppe et al., 2004b; Tafforeau et al., 2007). As a result, a significant attenuation of the amplitude of the isotopic input signals can occur in tooth enamel. To minimize signal attenuation, a few different sampling strategies have been proposed. For instance, Tafforeau et al. (2007) suggested sampling the innermost layer of enamel adjacent to the EDJ, which mineralizes during or just after the appositional phase. In contrast, Hoppe et al. (2004a) suggested milling along the Retzius striae, i.e., parallel to appositional microtextures. However, we did not follow these sampling strategies for various reasons. With respect to sampling the enamel layer adjacent to the EDJ, studies performed on rhinoceros enamel showed that this layer is very thin (~20 μm) (Tafforeau et al., 2007). Therefore, isolating this layer would be very challenging and *in situ* analysis at high spatial resolutions would require instruments available only in few institutions, i.e., secondary ion mass spectrometry or SIMS (Blumenthal et al., 2014). An additional problem in using SIMS for isotopic analyses of fossil tooth enamel is that this technique analyzes the oxygen coming from all the oxygen-bearing components of hydroxyapatite (i.e., the phosphate, carbonate, and hydroxyl components) and the hydroxyl ion is readily altered by diagenesis (Kohn et al., 1999). Finally, while *in situ* sampling of the innermost enamel layer can reduce signal dampening due to sampling and maturation, no sampling method can remove the other sources of attenuation (i.e., body fluid reservoir effects and drinking from large water bodies). With respect to sampling strategies that follow appositional geometries, a recent study indicated that only the maturation phase is recorded in the isotopic composition of enamel; for this reason sampling strategies based on incremental features are currently not recommended (Trayler and Kohn, 2017). As a result, we implemented a conventional sampling technique that consisted in removing 2-3 mm-wide vertical strips of enamel with a slow speed diamond wafering saw and in sequentially sub-sampling the strips perpendicularly to the growth axis at intervals of 1.25 or 2.5 mm. We do not expect a significant effect of sample spacing on our data as a recent study showed that sampling at different intervals (up to 3 mm) does not affect the shape and patterns of intra-tooth isotopic profiles (Buchan et al., 2016). Following sub-sampling, we removed the dentine adhering to enamel with a razor blade under a binocular microscope. We also removed the outer layer of enamel with a dental drill. Because this layer mineralizes after the inner and central ones, its removal likely reduces the attenuation of the isotopic signal that is associated with enamel maturation (Trayler and Kohn, 2017).

3.4. Sample processing and isotopic analyses

Before the analyses of the carbonate component of enamel, powdered samples were treated with hydrogen peroxide to remove organic contaminants and with an acetic acid-calcium acetate solution to remove diagenetic carbonates (Crowley and Wheatley, 2014; Koch et al., 1997). After the treatment, the enamel samples were dissolved in phosphoric acid and analyzed in the SIRFER lab of the University of Utah with a Thermo Finnigan Delta Plus Isotope Ratio Mass Spectrometer connected to a Thermo Finnigan GasBench II. The carbon and oxygen isotope compositions were referenced to the V-PDB international standard using a two-point normalization based on the Carrara Marble ($\delta^{13}C = 2.09‰$, $\delta^{18}O = -1.85‰$ vs. V-PDB) and LSVEC ($\delta^{13}C = -46.6‰$, $\delta^{18}O = -26.7‰$ vs. V-PDB) primary standard reference materials. NBS 19 ($\delta^{13}C = 1.95‰$, $\delta^{18}O = -2.2‰$ vs. V-PDB) was used as a secondary standard reference material for quality control. The $\delta^{18}O$ values were converted from the V-PDB to the V-SMOW international standard using the following equation (Coplen et al., 1983):

$$\delta^{18}O_{V-SMOW} = 1.03091 \times \delta^{18}O_{V-PDB} + 30.91 \quad (7)$$

The within-run precision (± 1 σ) of these analyses as determined by the replicate analyses of NBS 19 was less than ± 0.2‰ for $\delta^{13}C$ and ± 0.3‰ for $\delta^{18}O$ (n = 3–8).

4. Results

As our sample set is comprised of teeth with different mineralization times and different tooth wear stages, we pooled all the data for each site and discuss them in terms of average values for ILP and GSN irrespective of their layer of provenance. This approach minimizes the effect of oversampling a given season and provides a number of samples that likely exceeds (in the case of ILP) or closely approaches (for GSN) that required to accurately reconstruct paleoclimates and paleoenvironments (Hoppe et al., 2005).

Tables S1 and S2 report the whole dataset of the study while Table 1 reports summary descriptive statistics for the δ-values of the analyzed teeth. We used two-tailed heteroscedastic t-tests to compare the means of two populations. Statistical significance is based on $p < 0.05$.

4.1. Enamel δ-values

Enamel $\delta^{13}C$ values of all sequential samples from ILP range from −15.1‰ to −12.5‰ and average −13.6 ± 0.5‰ (all averages are reported ± 1 σ). At GSN, $\delta^{13}C$ values range from −13.6‰ to −11.5‰ and average −12.1 ± 0.4‰. The average $\delta^{13}C$ value for ILP is significantly lower than that for GSN ($p < 0.01$, *t*-test; Fig. 6). Intra-tooth variability in enamel $\delta^{13}C$ is low at both ILP and GSN (Figs. 4 and 5); the average intra-tooth range is 0.9‰ at both sites.

Enamel $\delta^{18}O$ values of all sequential samples from ILP range from 22.3‰ to 26.1‰ and average 24.2 ± 0.7‰. At GSN, $\delta^{18}O$ values range from 23.4‰ to 26.0‰ and average 25.0 ± 0.6‰. The average $\delta^{18}O$ value for ILP is significantly lower than that for GSN ($p < 0.01$, *t*-test; Fig. 7). Intra-tooth variability in enamel $\delta^{18}O$ is moderate at both sites (Figs. 4 and 5); the average intra-tooth range is 1.9‰ at ILP and 1.7‰ at GSN.

5. Discussion

5.1. Middle Pleistocene paleoenvironments and paleoclimate

As expected, all the investigated rhinoceros teeth have enamel $\delta^{13}C$ values lower than −6.8‰, which indicate feeding in a pure C_3 ecosystem. Similar to the modern environments (Collins and Jones, 1986), there is no evidence for C_4 plants in the area during the Middle Pleistocene. At ILP, 2 out of 257 enamel samples have a $\delta^{13}C$ lower than −14.9‰, indicating that one rhinoceros individual may have partially fed in closed canopy forests ~600 ka. In contrast, at GSN, none of the enamel samples has a $\delta^{13}C$ lower than −14.9‰, so there is no evidence for feeding in closed canopy forests ~400 ka. At both sites, there is no evidence for feeding in open woodlands and/or xeric C_3 grasslands, as none of the enamel samples has a $\delta^{13}C$ between −9.7 and −6.8‰. These results are consistent with mesowear and anatomical studies conducted on both rhinoceros species, which suggest high dietary flexibility, particularly for *S. hundsheimensis* (Kahlke and Kaiser, 2011; van Asperen and Kahlke, 2015). Assuming that the rhinoceroses' diet is

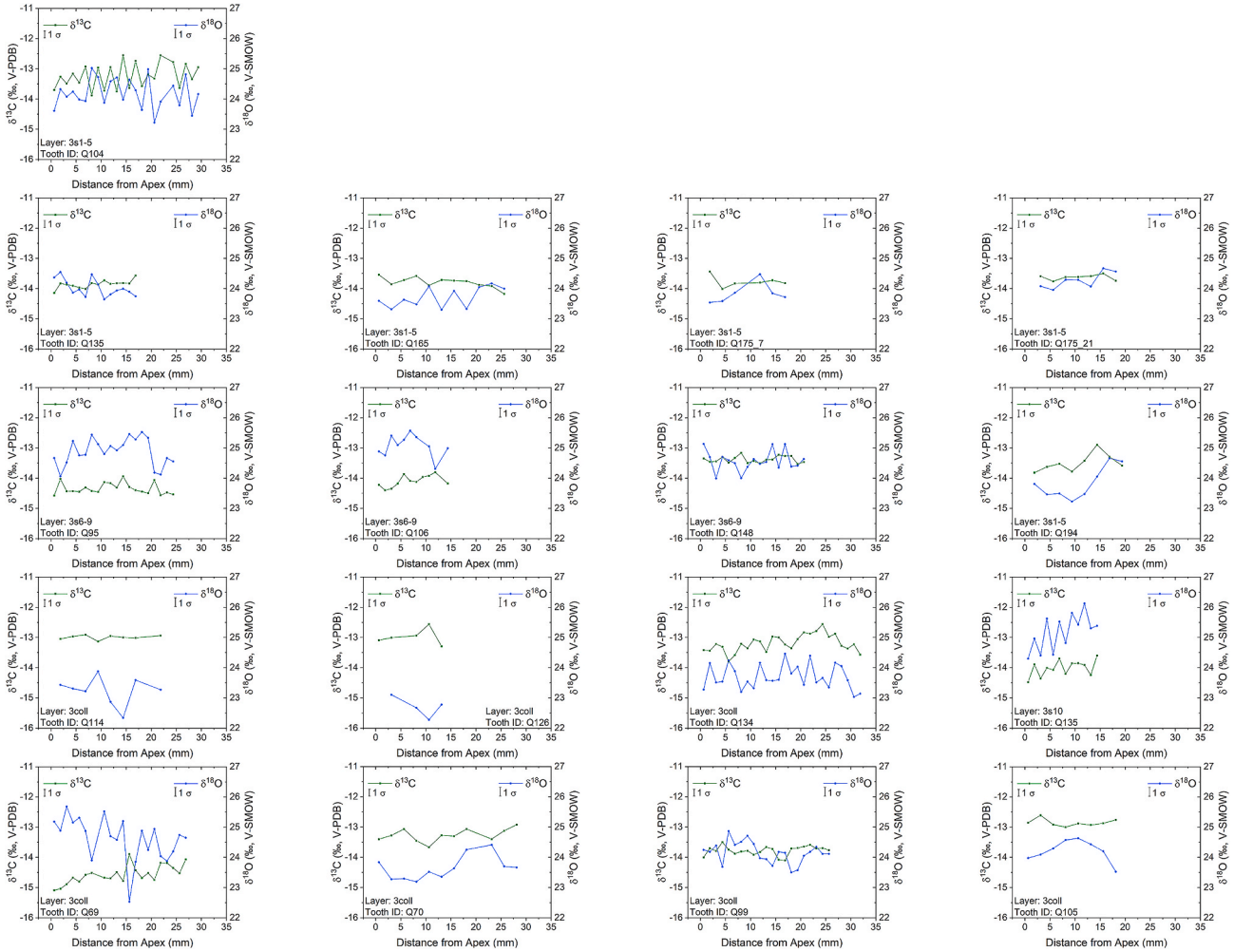

Fig. 4. Rhinoceros tooth enamel $\delta^{13}C$ and $\delta^{18}O$ values vs. distance from the top of the tooth for the four sampled stratigraphic layers of Isernia La Pineta. 1 σ error bars represent within-run variations on standards. Most of the intra-tooth profiles show a small variability in $\delta^{13}C$ and a moderate variability in $\delta^{18}O$, suggesting low precipitation seasonality and moderate temperature seasonality ~600 ka.

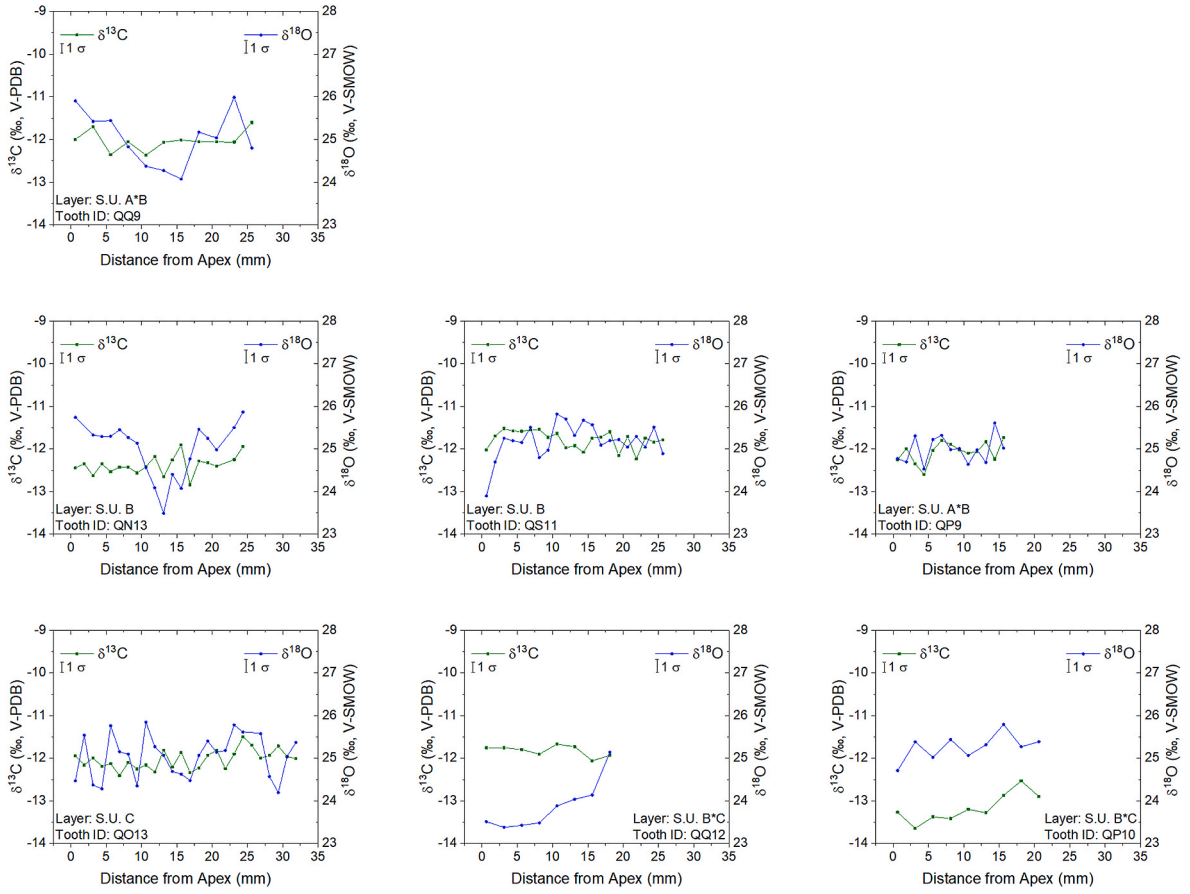

Fig. 5. Rhinoceros tooth enamel $\delta^{13}C$ and $\delta^{18}O$ values vs. distance from the top of the tooth for the four sampled stratigraphic layers of Guado San Nicola. 1 σ error bars represent within-run variations on standards. Most of the intra-tooth profiles show a small variability in $\delta^{13}C$ and a moderate variability $\delta^{18}O$, suggesting low precipitation seasonality and moderate temperature seasonality ~400 Ka.

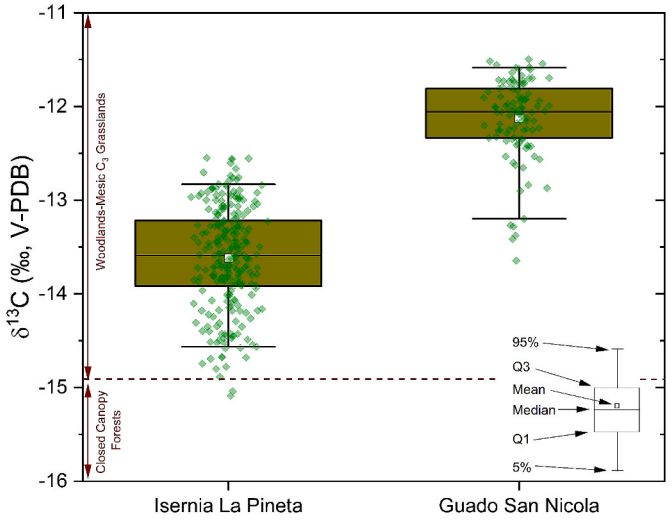

Fig. 6. Rhinoceros tooth enamel $\delta^{13}C$ values with box and whiskers plots for all the analyzed samples from Isernia la Pineta (ILP; ~600 ka) and Guado San Nicola (GSN; ~400 ka). At both ILP and GSN, enamel $\delta^{13}C$ values indicate feeding in a pure C_3 ecosystem that consisted mostly of woodlands and/or mesic C_3 grasslands with the possible sparse presence of closed canopy forests at ILP. Enamel from ILP shows a lower average $\delta^{13}C$ value than enamel from GSN, suggesting higher mean annual precipitation and lesser aridity ~600 vs. ~400 ka.

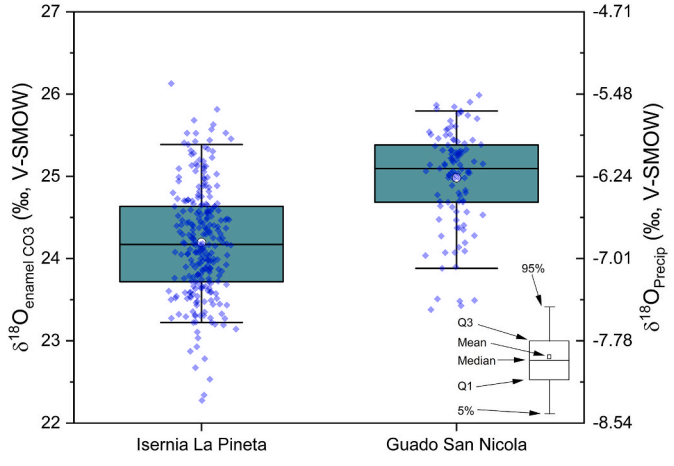

Fig. 7. Rhinoceros tooth enamel carbonate $\delta^{18}O$ values with box and whiskers plots for all the analyzed samples from Isernia la Pineta (ILP, ~600 ka) and Guado San Nicola (GSN, ~400 ka). On the y-axis on the right, we show the $\delta^{18}O$ values of meteoric precipitation ($\delta^{18}O_{precip}$) calculated from enamel compositions with the equation of Tütken et al. (2006). Enamel from ILP shows a slightly lower average $\delta^{18}O$ than enamel from GSN, likely reflecting the higher elevation of ILP, lesser aridity and/or lower mean annual temperature ~600 vs. 400 ka.

representative of the average vegetation of the area (i.e., no diet or niche selectivity), enamel $\delta^{13}C$ values at both sites suggest that the dominant ecosystem consisted of woodlands and/or mesic C_3 grasslands.

To calculate precipitation amounts, we applied the relationship between the $\delta^{13}C$ of modern C_3 plants and MAP developed Kohn (2010):

$$MAP\left(\frac{mm}{yr}\right) = 10^{\frac{\delta^{13}C_{plants}+10.29+(0.0124\times Abs.\ \ Latitude)-\left(1.9\times10^{-4}\times Altitude\right)}{5.61}} - 300 \quad (8)$$

$\delta^{13}C_{plants}$ was calculated from enamel $\delta^{13}C$ using equation (4) and by correcting for the lower $\delta^{13}C$ of atmospheric CO_2 during the Middle Pleistocene relative to the modern value:

$$\delta^{13}C_{plants} = \frac{1000\times(\delta^{13}C_{enamel}-14.5)}{14.5+1000} - 1 \quad (9)$$

$\delta^{13}C$ values of C_3 plants are independent of atmospheric CO_2 concentrations (Kohn, 2016) so it is not necessary to correct for the different pCO_2 at ~600 and ~400 ka relative to the modern value. Similarly, uncertainties in altitude do not strongly affect the carbon isotope composition of the plants, therefore possible differences between the Middle Pleistocene and modern elevations of the two sites are unlikely to have an effect on calculated MAP's (Kohn, 2010). We calculated MAP's from the average enamel $\delta^{13}C$ of the two sites and with an uncertainty given by the 2 se (i.e., uncertainties include only compositional variability). The results for ILP (1290 ± 44 mm/yr) and GSN (570 ± 30 mm/yr) suggest higher MAP and lesser aridity ~600 vs. ~400 ka. With respect to seasonal changes, the low intra-tooth variability in enamel $\delta^{13}C$ likely indicates a lack of seasonal variation in the diet and a uniform carbon isotope composition of the plants throughout the year, implying low seasonality in the amounts of meteoric precipitation. However, the low variability may also reflect time-averaging and amplitude attenuation of the isotopic signal of the plants due to the long process of enamel mineralization.

Enamel carbonate $\delta^{18}O$ values can be used to estimate the oxygen isotope composition of meteoric precipitation at ILP and GSN ~600 and ~400 ka. The main assumption behind this approach is that the composition of the rhinoceroses' drinking water is representative of the average composition of local meteoric precipitation. This assumption can be violated under the following scenarios: 1) when evaporation modifies the original isotopic signal of surface (drinking) water, leading to an increase in its $\delta^{18}O$ value (Craig and Gordon, 1965); 2) when surface water interacts with water from aquifers that are recharged preferentially during a given season. For instance, interaction with groundwater that is preferentially recharged during the winter (when precipitation in the area is currently more abundant) would lower the composition of surface water bodies relative to the average composition of meteoric precipitation (Clark and Fritz, 1997); 3) when surface water in lakes and streams originates from areas of higher elevation; in this case $\delta^{18}O$ values would be again lower than the average value of local meteoric precipitation (for a quantification of the altitude effect in Molise see Petrella et al., 2009); and 4) when animals migrate seasonally to escape harsh winter conditions and ingest meteoric waters with higher $\delta^{18}O$ that falls in areas with higher temperatures (Feranec et al., 2009; Julien et al., 2012).

We consider scenario 1 unlikely considering the $\delta^{13}C$ data, which suggest that the rhinoceroses inhabited humid and relatively closed habitats where evaporation is expected to be low. The likelihood of scenarios 2–4 is more difficult to evaluate. The modern average isotopic composition of groundwater from Longano (which is ~10 km from ILP and GSN) (Fig. 1) is ~1‰ lower than the average isotopic composition of meteoric precipitation from the same site, suggesting that currently winter precipitation slightly dominates aquifers recharge (Petrella and Celico, 2013). Our data, however, seem to indicate lower precipitation seasonality in the Middle Pleistocene, so recharge may have been more uniform at that time. With respect to migrations, strontium isotope analyses of teeth from ILP seems to suggest seasonal migrations of small distances (~50–150 km; Lugli et al., 2017). Seasonally migrating animals, however, typically show low intra-tooth variability in $\delta^{18}O$ and high intra-tooth variability in $\delta^{13}C$ (Feranec et al., 2009; Harris et al., 2020; Julien et al., 2012), in direct contrast to our results. Our study is consistent with that of Lugli et al. (2017) if seasonal migrations occurred, but the rhinoceroses moved only to nearby areas having an isotopic composition of precipitation very similar to that of ILP and GSN. Finally, from our data we cannot rule out the possibility that some rhinoceros individuals partially ingested meteoric waters coming from areas of higher elevations than that of our two study sites. However, our large sample size should allow the resulting lower $\delta^{18}O$ values to be averaged out.

If the assumption holds, the $\delta^{18}O$ of meteoric precipitation ($\delta^{18}O_{precip}$) can be calculated from the composition of enamel carbonate ($\delta^{18}O_{enamel\ CO3}$) by applying the equation ($R^2 = 0.94$) obtained for modern rhinoceroses by Tütken et al. (2006):

$$\delta^{18}O_{precip} = (0.77\pm0.14)\times\delta^{18}O_{enamel\ \ CO3} - (25.41\pm3.75) \quad (10)$$

It is noteworthy that while Tütken et al. (2006) provided this equation as $\delta^{18}O_{precip}$ vs. $\delta^{18}O_{enamel\ PO4}$, we report it here in its original form (i.e., as $\delta^{18}O_{precip}$ vs. $\delta^{18}O_{enamel\ CO3}$). The application of this equation gives average values for the $\delta^{18}O$ of meteoric precipitation at ILP and GSN of −6.8 ± 5.1‰ and −6.2 ± 5.1‰, respectively. These values are essentially identical to the modern annual average value (−6.8‰) at Longano (Giustini et al., 2016). In addition, our calculated values are also indistinguishable from those obtained for ILP (−6.7‰) and GSN (−6.3‰) with the Online Isotopes in Precipitation Calculator (Bowen, 2009).

Several complications exist in calculating MAT from these $\delta^{18}O_{precip}$ values. Firstly, while in most mid-latitude locations the isotopic composition of meteoric precipitation shows a strong correlation with temperature (Rozanski et al., 1993), this correlation is very weak in Italy due to its complex topography and climate (Longinelli and Selmo, 2003). Secondly, the use of transposed vs. inverted forward regression fits for paleotemperature reconstructions is currently under debate (Pryor et al., 2014; Skrzypek et al., 2016). Lastly, the correlation between $\delta^{18}O_{precip}$ and MAT is not necessarily constant in time and the temporal temperature sensitivity in the $\delta^{18}O$ of meteoric precipitation is not necessarily the same as the modern spatial temperature sensitivity that is often used in paleotemperature reconstructions. For these reasons, we will not attempt to calculate absolute values of MAT here. However, despite these complications, the similarity between the $\delta^{18}O_{precip}$ values calculated for our Middle Pleistocene sites and the modern values suggests that MAT's were broadly similar to today (i.e., ~13°C). The lower average enamel $\delta^{18}O$ of ILP relative to GSN is likely caused by the difference in elevation between the two sites and perhaps by slightly lower MAT in the region ~600 vs. ~400 ka. The increased aridity ~400 compared to ~600 ka could also explain, at least in part, the higher average enamel $\delta^{18}O$ of GSN, although rhinoceros enamel $\delta^{18}O$ seems not to be very sensitive to changes in aridity (Levin et al., 2006).

With respect to temperature seasonality, the moderate intra-tooth variability in enamel $\delta^{18}O$ likely indicates moderate seasonal contrasts in temperature. More specifically, the average intra-tooth range in enamel $\delta^{18}O$ from ILP and GSN (~2‰) is higher than that observed for modern and Miocene rhinoceroses from tropical locations (1–1.9‰) (MacFadden and Higgins, 2004; Martin et al., 2008; Zin Maung Maung et al., 2011) and from the SE US (1.1–1.3‰) (DeSantis and Wallace, 2008), but is lower than that for Miocene-Pliocene rhinoceroses from continental China (2.0–2.5‰) (Biasatti et al., 2018; Ciner et al., 2015; Zhang et al., 2012) and for Eocene, Oligocene, and Miocene rhinoceroses from continental North America (2.2–3.9‰) (Harris et al., 2020; Zanazzi et al., 2015; Zanazzi and Kohn, 2008). These observations suggest a moderate MART of perhaps 10–20°C for ILP and GSN, similar or slightly lower than the modern value.

Table 2
Results of selected paleoclimatic and paleoenvironmental studies conducted on Middle Pleistocene terrestrial sections in central and southern Italy. MIS: marine isotope stage; MAP: mean annual precipitation; MAT: mean annual temperature.

Site	Age	MIS	Proxy	Paleoenvironment	MAP	MAT	Other Climatic Parameters	Reference
Isernia La Pineta	587-583 ka	15	Stable isotopes in rhinoceros tooth enamel	Woodlands and/or mesic grasslands, possibly sparse closed canopy forests	~1300 mm/yr	Similar to modern (~13°C)	Moderate temperature seasonality and low precipitation seasonality	This study; Peretto et al. (2015a)
Guado San Nicola	400-345 ka	11	Stable isotopes in rhinoceros tooth enamel	Woodlands and/or mesic grasslands	~600 mm/yr	Similar to modern (~13°C)	Moderate temperature seasonality and low precipitation seasonality	This study; Peretto et al. (2015b)
Grotta Romanelli	Pleistocene (630 ka?)	16?	Stable isotopes in rhinoceros tooth enamel	Woodlands and/or mesic grasslands	220–460 mm/yr	15.5–17.2°C		Pandolfi et al. (2018)
Isernia La Pineta	587-583 ka	15	Faunal analysis	Closed forests, semi-open woodlands, grasslands		0.98°C (?)		Alhaique et al. (2004); Montuire and Marcolini (2002); Orain et al. (2013b); Peretto et al. (2004, 2015a); Thun Hohenstein et al. (2004, 2009)
Notarchico	670-614 ka	16	Faunal analysis	Closed forests, semi-open woodlands, grasslands		9.17°C		Montuire and Marcolini (2002); Sardella et al. (2006); Pereira et al. (2015); Orain et al. (2013b)
Guado San Nicola	400-345 ka	11	Faunal analysis	Open woodlands, closed grasslands, punctually local forests				Orain et al. (2013b); Peretto et al. (2015b)
Torre in Pietra	Middle Pleistocene	9 and 7	Faunal analysis	Closed forests, open woodlands, grasslands		11.9°C (MIS 7)		Radmilli and Boschian (1996); Caloi et al. (1998); Montuire and Marcolini (2002); Sardella et al. (2006); Palombo and Sardella (2007); Boschian and Saccà (2010); Anzidei et al. (2012), Orain et al. (2013b)
Cava Campani	Middle Pleistocene (620–460 ka?)	15-12?	Faunal analysis	Woodlands		11.9°C		Marcolini et al. (2001); Montuire and Marcolini (2002)
Boiano	>426–15 ka	13–2	Pollen analysis	Coniferous and deciduous forests during interglacials, steppe during glacials	~900 mm/yr (MIS 11)		$T_{January}$ ~ -2°C, P_{winter}~200 mm/yr, P_{summer}~200 mm/yr (MIS 11)	Orain et al. (2012); Orain et al. (2013a); Orain et al. (2013b); Combourieu-Nebout et al. (2015)
Sessano	600-400 ka	15–12	Pollen analysis	Deciduous forests during interglacials, steppe during glacials				Ermolli et al. (2010); Amato et al. (2011); Combourieu-Nebout et al. (2015)
Vallo di Diano	650-450 ka	16–13	Pollen analysis	Deciduous forests during interglacials, steppe during glacials	~700–1000 mm/yr (MIS 15); ~700 mm/yr (MIS 15–13)	~-13°C (MIS 15)	$T_{January}$ = 4°C, T_{July} = 22°C (MIS 15); $T_{January}$~2°C, P_{winter}~200 mm/yr, P_{summer}~150 mm/yr (MIS 15–13)	Ermolli (1996); Ermolli et al. (1995); Ermolli and Cheddadi (1997); Karner et al. (1999); Combourieu-Nebout et al. (2015)

Our paleoenvironmental and paleoclimatic reconstruction is supported by the majority of pollen and faunal studies from terrestrial Middle Pleistocene contexts in central and southern Italy (Table 2). With respect to pollen studies, the only records that overlap in age with ILP and GSN are Vallo di Diano, Boiano, and Sessano. The MIS 15-MIS 12 deposits of Valle Gumentina have unfortunately scarce and poorly preserved pollen grains (Villa et al., 2016). At Vallo di Diano, which is further south in Campania (Fig. 1), reconstructions based on the best modern analog method indicate a MAP of 700–1000 mm/yr and a MAT of 8–13°C during MIS 15 (Ermolli and Cheddadi, 1997). Based on the same pollen assemblage, Combourieu-Nebout et al. (2015) report a MAP of 700 mm/yr for MIS 15-MIS 13. MIS 15 and MIS 11 are characterized by the abundant presence of *Abies* at Sessano and Boiano, respectively. *Abies alba* lives today in areas where MAP is higher than 1000 mm/yr and where MAT is 6–16°C (Di Rita and Sottili, 2019). The abundant presence of this genus at this site therefore suggests temperate and wet conditions but can also be explained by the richness of clay in the Molise soils (Ermolli et al., 2015). *Cedrus* has less strict climatic requirements (MAT = 7–18°C, MAP = 500–1500 mm/yr) (Ermolli et al., 2010) and the few grains present at Boiano, Sessano, and Vallo di Diano may have been transported from Africa. Some support for a wet climate comes from Combourieu-Nebout et al. (2015), who report a MAP of ~900 mm/yr for MIS 11 at Boiano. It is noteworthy, however, that Boiano is characterized by unique edaphic and microclimatic conditions, (Orain et al., 2012, 2013a), and for this reason its record is difficult to compare with those from other sites. With respect to faunal studies, Montuire and Marcolini (2002) report an unrealistic MAT of 0.98°C for ILP, which likely reflects the non-preservation or non-recovery of arvicolid species. Additional quantitative estimates of temperature and precipitation reported for the Middle Pleistocene include a MAT of ~12°C in Tuscany at the poorly dated site of Cava Campani and in the upper beds of Torre in Pietra, near Rome, during MIS 7 (Fig. 1) (Montuire and Marcolini, 2002). The same study also reports a MAT of ~9°C during MIS 16 at the archeological site of Notarchico in Basilicata (Fig. 1). Finally, $\delta^{18}O$ and $\delta^{13}C$ data from *Stephanorhinus* tooth enamel from Grotta Romanelli (Fig. 1) suggest a MAT and a MAP of ~16°C and ~350 mm/yr, respectively (Pandolfi et al., 2018). However, this site is located much further south in Apulia (Fig. 1) and is characterized by higher MAT and lower MAP in our modern climate (Brunetti et al., 2014; Crespi et al., 2018).

In terms of seasonality, pollen data from Vallo di Diano indicate uniform precipitation amounts (~200 mm in the winter and ~150 mm in the summer) during MIS 15-MIS 13 (Combourieu-Nebout et al., 2015), supporting our conclusion of low precipitation seasonality at ILP ~600 ka. Combourieu-Nebout et al. (2015) also infer low precipitation seasonality (~200 mm in both summer and winter) during MIS 11 from the Boiano pollen record, but the special characteristics of this site make a direct comparison with our data from GSN problematic. Precipitation seasonality was low also in Spain during a number of Middle Pleistocene interglacials, as revealed by a mutual climatic range study on herpetofaunal assemblages (Blain et al., 2012). Similarly, moderate temperature seasonality is supported by a pollen study conducted at Vallo di Diano where MART was estimated to be equal to ~18°C during MIS 15 (Ermolli and Cheddadi, 1997).

5.2. Implications for human migrations and evolution

The chronology of human dispersals from Africa and the colonization of Europe is one of the most debated topics in paleoanthropology (see review in Antón and Swisher, 2004; Carbonell et al., 2008). Until two decades ago, the widely accepted theory (named the "short chronology") was that hominins were restricted to Africa until 0.8 Ma (Roebroeks and Van Kolfschoten, 1994). Within this model, hominin migration to Europe was associated with the development of the Acheulean technology and the migrating human was widely considered to have been *Homo erectus*. This view is now considered to be incorrect following the discovery of sites like Dmanisi in Georgia (Gabunia et al., 2000), Pirro Nord and Cà Belvedere di Monte Poggiolo in Italy (Fig. 1) (Arzarello et al., 2007, 2012, 2014; Arzarello and Peretto, 2010; López-García et al., 2015b; Muttoni et al., 2011; Peretto et al., 1998); Sima del Elefante, Fuente Nueva, and Barranco Léon in Spain (Carbonell et al., 2008; De Castro et al., 2010; Lorenzo et al., 2015; Moyano et al., 2011; Toro-Moyano et al., 2009). The modern, generally accepted view (named the "long chronology") is that the initial human dispersal into Europe occurred much earlier and was not related to advancements in technology (Manzi et al., 2011). Two distinct waves of migrations are now hypothesized (Arsuaga et al., 1997; Carbonell et al., 2008; De Castro et al., 1997; Manzi et al., 2011). The first wave involved only archaic hominins (considered to have been *Homo ergaster/erectus*), it occurred earlier than 1.2 Ma, and was associated with Oldowan (or Mode I) technology. This technology involved simple lithic reduction strategies and the use of hammerstones to detach flakes from pebble cores. The second wave involved more encephalized humans (mostly referred to *Homo heidelbergensis*), was after 700 ka, and was usually (but not always) associated with Acheulan (or Mode II) technology (Antón and Swisher, 2004; Moncel, 2010). In contrast to the Oldowan, Acheulean technology involved more elaborate techniques to shape and retouch stones and to produce biface tools (e.g., hand axes). Possible migrations routes were the Strait of Gibraltar, Bab-el-Mandeb, Sicily, and the Levantine (or Palestine) Corridor (van der Made and Mateos, 2010). The Strait of Gibraltar is however considered an unlikely possibility because of the separation between Pleistocene African and European fauna, the lack of boat technology, and the difficulty of swimming in ocean waters (van der Made, 2005). The absence of post Miocene Red Sea land bridges would have made dispersal through Bab-el-Mandeb also problematic (Fernandes et al., 2006). Similarly, Sicily has been discarded from the possible migration routes because of the absence of human remains before the Upper Paleolithic and its endemic fauna (Villa, 2001). According to Holmes (2007), the most likely migration route was therefore the Levantine corridor. It is very likely that both of the migratory waves were controlled by the cyclic Pleistocene climate (Antón and Swisher, 2004; Muttoni et al., 2010), although the exact role of climate on waves of human migrations remains unclear (Agustí et al., 2009, 2010; Kahlke et al., 2011; Leroy et al., 2011; Messager et al., 2011; Saarinen et al., 2021).

Given its age and strategic geographic position between Africa and continental Europe, ILP is an ideal site to test the role of climate on early hominin migrations. Although at the current state of research it is impossible to say for sure whether evidence from ILP represents a secondary wave of migration rather than for the first occupants of the Italian peninsula, the lithic industry of ILP does not share the technological traits of the earlier Italian sites of Pirro Nord (dated to ~1.6–1.3 Ma) (Arzarello et al., 2012; López-García et al., 2015b) and Cà Belvedere di Monte Poggiolo (dated to ~1.0–0.85 Ma) (Muttoni et al., 2011; Peretto, 2006) and, more in general, of earlier sites in western Europe. More specifically, a recent study showed that the lithic industry of ILP is characterized by innovative technical features analogous to those of other well-dated and well-investigated penecontemporaneous (~0.8–0.6 Ma) sites in western Europe (Gallotti and Peretto, 2015). Therefore, accepting the chronology of Pirro Nord and Cà Belvedere di Monte Poggiolo, and considering the chronology and the archeological evidence of ILP (in particular the lithic industry), evidence for this site is likely ascribed to a second migration wave. If the record from ILP indeed represents a new wave of peopling and not a lag adaptation, the results of our study suggest that the sites of the second migration wave were favored by mild climatic conditions, similar to the sites of the first wave (Agustí et al., 2009, 2010; Kahlke et al., 2011). Several climatic and environmental features revealed by this study may have favored human migration and colonization. For instance, the environment was relatively open, a condition that favors migrations of large mammals and consequently of humans (van der Made and Mateos, 2010). The mosaic of biomes (woodlands, grasslands, closed canopy forests) dominated by

C_3 plants (which are more nutritious than C_4 grasses) likely offered copious amounts of food, including both browse (leaves, fruits) and graze (grasses) resources, that could accommodate various feeding styles. In addition, MAP was sufficient in overall amount and seasonal distribution to provide reliable food resources throughout the year but not high enough to develop dense and extensive forests that would have obstructed the movement of herbivore herds. Finally, the temperate climate with moderate seasonal contrasts likely favored the survival of these early hominins (which did not yet have the control of fire) by limiting the occurrence of frost conditions and the extent and duration of the snow cover.

Following the colonization of the peninsula by early hominins, the period represented by the GSN sediments was crucial from a human evolution perspective as it was marked by the development in western Europe of tools made from flakes detached from prepared cores, a technique called the Levallois or Mode III (Moncel, 2010). In contrast to the Acheulian, Levallois technology involves a hierarchical core reduction strategy and the multistage shaping of a mass of stone (the core) in preparation to detach a flake of predetermined size and shape. Whereas flakes resulting from biface production were treated as waste in the Acheulian, these flakes are the desired product in Levallois technology. The development of Levallois technology in Europe marked the transition from the Lower to the Middle Paleolithic and documents the most important conceptual shift in stone tool production strategies since the demise of the Oldowan technology (Adler et al., 2014). This transition was also marked by other significant behavioral and anatomical innovations among hominin populations, including, for example, the use of fire, the manipulation of pigments, the mastery of hafting, more elaborate hunting strategies, and the first appearance of early Neanderthal morphological features (Hublin, 2009; Moncel et al., 2020; Picin et al., 2013).

Well-dated sites like GSN offer the unique opportunity to investigate the relationship between climatic and environmental change and evolution in the hominin clade. Similar to East Africa, where hominin speciation, the emergence of Oldowan and Acheulian tool industries, and the development of meat eating have been associated with increased aridity (Potts, 2013), the climate change event towards more arid conditions that occurred sometime between ~600 and ~400 ka in central Italy might have played a role in the technological and cultural evolution of hominins that occurred at that time and in the appearance of prepared-core tools at GSN. As suggested by Owen et al. (2018) and Potts et al. (2018), increases in aridity produce less predictable and more heterogeneous distribution of resources in the landscape. The extensional tectonic activity that occurred in the region during the Middle Pleistocene and the consequential formation of several inter montane basins (Cavinato and Celles, 1999; Corrado et al., 1997; Di Bucci et al., 2002), would have provided additional landscape fragmentation. In turn, an uneven distribution of resources favors wider mobility and more information gathering and investment in social interactions, processes that favor technological change and its dissemination (Owen et al., 2018; Potts et al., 2018). Precipitation amount drives natural selection (Siepielski et al., 2017), therefore increased aridity may have also operated directly, for example, by selecting for cognitive abilities to produce and transport increasingly diversified toolkits over greater distances. Additional high-resolution paleoclimate reconstructions from well-dated Italian sites of similar age are required to investigate whether the increase in aridity recorded in our data was an abrupt event or whether it was part of a long-term trend possibly associated with short-term wet-dry fluctuations.

6. Conclusions

New data are presented here on the carbon and oxygen stable isotope composition of rhinoceros (*Stephanorhinus* spp.) tooth enamel from Isernia La Pineta (ILP, ~600 ka) and Guado San Nicola (GSN, ~400 ka), two key Middle Pleistocene sites located in the Molise region of central Italy. These data are used to provide a reconstruction of the paleoclimate and paleoenvironment of the two sites during periods of hominin occupation. Our data suggest that:

1) *Stephanorhinus* was feeding in pure C_3 ecosystems. Similar to modern environments, there is no evidence of C_4 plants at the two sites ~600 and ~400 ka.
2) The ecosystems were dominated by woodlands and/or mesic C_3 grasslands, with the possible sparse presence of closed canopy forests at or near ILP ~600 ka. Mean annual precipitation decreased and aridity markedly increased from ~600 to ~400 ka.
3) The oxygen isotope compositions of meteoric precipitation calculated from enamel data are very similar to the modern values, suggesting that mean annual temperatures ~600 and ~400 ka were broadly similar to today (~13°C).
4) Precipitation seasonality was likely low and temperature seasonality was likely moderate both ~600 and ~400 ka.
5) The mosaic of ecosystems and the relatively warm, wet, and seasonally uniform climate of ILP might have favored the second wave of human migrations to Europe by providing an environment suitable for the movement of large mammal herds, by offering abundant food year-round, and by limiting the occurrence of frost conditions. The increase in aridity that occurred sometime between ~600 and ~400 ka might have favored the dissemination of technological innovations in the area by creating more heterogeneous landscape resources that forced hominins to travel more widely and to interact more with other groups.

Author contributions

Alessandro Zanazzi: Conceptualization, Methodology, Validation, Formal Analysis, Data Curation, Writing-Original Draft, Writing-Review & Editing, Visualization, Supervision, Project Administration, Funding Acquisition. Andrew Fletcher: Investigation, Funding Acquisition. Carlo Peretto: Resources, Supervision, Project Administration. Ursula Thun Hohenstein: Resources, Supervision, Project Administration.

Data availability

Supplementary data related to this article are found in Tables S1 and S2 at https://doi.org/10.1016/j.quaint.2022.01.011.

Declaration of competing interest

The authors declare that they have no known competing financial interests or personal relationships that could have appeared to influence the work reported in this paper.

Acknowledgements

The authors thank Suvankar Chakraborty for performing the isotope analyses, Thomas Tütken for providing the modern rhinoceroses data, Giuseppe Lembo and Weihong Wang for helping with the figures, Benedetto Sala, Marta Arzarello, Claudio Berto, Matthew Kohn and two anonymous reviewers for their helpful comments and suggestions. The project was funded by the UVU grants GEL 605 and 589 (to AZ); SAC SHS065 (to AF) and SHF010 (to AZ).

Appendix A. Supplementary data

Supplementary data to this article can be found online at https://doi.org/10.1016/j.quaint.2022.01.011.

References

Adler, D.S., Wilkinson, K., Blockley, S., Mark, D., Pinhasi, R., Schmidt-Magee, B., Nahapetyan, S., Mallol, C., Berna, F., Glauberman, P., 2014. Early Levallois technology and the lower to middle Paleolithic transition in the southern caucasus. Science 345, 1609–1613.

Agustí, J., Blain, H.-A., Cuenca-Bescós, G., Bailon, S., 2009. Climate forcing of first hominid dispersal in Western Europe. J. Hum. Evol. 57, 815–821.

Agustí, J., Blain, H.-A., Furió, M., De Marfá, R., Santos-Cubedo, A., 2010. The early Pleistocene small vertebrate succession from the Orce region (Guadix-Baza Basin, SE Spain) and its bearing on the first human occupation of Europe. Quat. Int. 223–224, 162–169.

Agustí, J., Lordkipanidze, D., 2019. An alternative scenario for the first human dispersal out of Africa. L'Anthropologie 123, 682–687.

Aiello, L.C., Dunbar, R.I., 1993. Neocortex size, group size, and the evolution of language. Curr. Anthropol. 34, 184–193.

Aiello, L.C., Wheeler, P., 1995. The expensive-tissue hypothesis: the brain and the digestive system in human and primate evolution. Curr. Anthropol. 36, 199–221.

Amato, V., Aucelli, P., Cesarano, M., Pappone, G., Rosskopf, C.M., Ermolli, E.R., 2011. The Sessano intra-montane basin: new multi-proxy data for the Quaternary evolution of the Molise sector of the Central-Southern Apennines (Italy). Geomorphology 128, 15–31.

Alhaique, F., Bisconti, M., Castiglioni, E., Cilli, C., Fasani, L., Giacobini, G., Grifoni, R., Guerreschi, A., Iacopini, A., Malerba, G., Peretto, C., Recchi, A., Rocci Riss, A., Ronchitelli, A., Rottoli, M., Thun Hohenstein, U., Tozzi, C., Visentini, P., Wilkens, B., 2004. Animal resources and subsistence strategies. Coll. Antropol. 28 (1), 23–40.

Amato, V., Aucelli, P.P., Cesarano, M., Jicha, B., Lebreton, V., Orain, R., Pappone, G., Petrosino, P., Ermolli, E.R., 2014. Quaternary evolution of the largest intermontane basin of the Molise Apennine (central-southern Italy). Rendiconti Lincei 25, 197–216.

Antón, S.C., Swisher III, C.C., 2004. Early dispersals of Homo from Africa. Annu. Rev. Anthropol. 33, 271–296.

Anzidei, A.P., Bulgarelli, G.M., Catalano, P., Cerilli, E., Gallotti, R., Lemorini, C., Milli, S., Palombo, M.R., Pantano, W., Santucci, E., 2012. Ongoing research at the late Middle Pleistocene site of La Polledrara di Cecanibbio (central Italy), with emphasis on human–elephant relationships. Quat. Int. 255, 171–187.

Arobba, D., Boscato, P., Boschian, G., Falgueres, C., Fasani, L., Peretto, C., Sala, B., Thun Hohenstein, U., Tozzi, C., 2004. Palaeoenvironmental analysis. Coll. Antropol. 28 (1), 5–21.

Arsuaga, J.L., Martınez, I., Gracia, A., Lorenzo, C., 1997. The Sima de los Huesos crania (Sierra de Atapuerca, Spain). A comparative study. J. Hum. Evol. 33, 219–281.

Arzarello, M., Marcolini, F., Pavia, G., Pavia, M., Petronio, C., Petrucci, M., Rook, L., Sardella, R., 2007. Evidence of earliest human occurrence in Europe: the site of Pirro Nord (southern Italy). Naturwissenschaften 94, 107–112.

Arzarello, M., Pavia, G., Peretto, C., Petronio, C., Sardella, R., 2012. Evidence of an early Pleistocene hominin presence at Pirro Nord (Apricena, Foggia, southern Italy): P13 site. Quat. Int. 267, 56–61.

Arzarello, M., Peretto, C., 2010. Out of Africa: the first evidence of Italian peninsula occupation. Quat. Int. 223, 65–70.

Arzarello, M., Peretto, C., Moncel, M.-H., 2014. The Pirro Nord site (Apricena, Fg, southern Italy) in the context of the first European peopling: convergences and divergences. Quat. Int. 389, 255–263.

Balasse, M., 2002. Reconstructing dietary and environmental history from enamel isotopic analysis: time resolution of intra-tooth sequential sampling. Int. J. Osteoarchaeol. 12, 155–165.

Ballatore, M., Breda, M., 2013. *Stephanorhinus hundsheimensis* (Rhinocerontidae, Mammalia) teeth from the early middle Pleistocene of Isernia La Pineta (Molise, Italy) and comparison with coeval British material. Quat. Int. 302, 169–183.

Belmaker, M., 2010. Early Pleistocene Faunal Connections between Africa and Eurasia: an Ecological Perspective. In: Out of Africa I. Springer, pp. 183–205.

Belmaker, M., 2011. On the Road to China: the Environmental Landscape of the Early Pleistocene in Western Eurasia and its Implication for the Dispersal of Homo, Asian Paleoanthropology. Springer, pp. 31–40.

Biasatti, D., Wang, Y., Deng, T., 2018. Paleoecology of Cenozoic rhinos from northwest China: a stable isotope perspective. Vertebr. Palasiat. 56, 45–68.

Blain, H.-A., Cuenca-Bescós, G., Lozano-Fernández, I., López-García, J.M., Ollé, A., Rosell, J., Rodríguez, J., 2012. Investigating the mid-Brunhes event in the Spanish terrestrial sequence. Geology 40, 1051–1054.

Blumenthal, S.A., Cerling, T.E., Chritz, K.L., Bromage, T.G., Kozdon, R., Valley, J.W., 2014. Stable isotope time-series in mammalian teeth: in situ $\delta^{18}O$ from the innermost enamel layer. Geochem. Cosmochim. Acta 124, 223–236.

Blumenthal, S.A., Levin, N.E., Brown, F.H., Brugal, J.P., Chritz, K.L., Harris, J.M., Jehle, G.E., Cerling, T.E., 2017. Aridity and hominin environments. Proc. Natl. Acad. Sci. U.S.A. 114, 7331–7336.

Bonnefille, R., 2010. Cenozoic vegetation, climate changes and hominid evolution in tropical Africa. Global Planet. Change 72, 390–411.

Boschian, G., Saccà, D., 2010. Ambiguities in human and elephant interactions? Stories of bones, sand and water from Castel di Guido (Italy). Quat. Int. 214, 3–16.

Bowen, G.J., 2009. The Online Isotopes in Precipitation Calculator, Version 2.2.

Bramble, D.M., Lieberman, D.E., 2004. Endurance running and the evolution of *Homo*. Nature 432, 345–352.

Brancaccio, L., Cinque, A., Di Crescenzo, G., Santangelo, N., Scarciglia, F., 1997. Alcune osservazioni sulla tettonica quaternaria nell'alta valle del f. Volturno (Molise). Il Quat. 10, 321–328.

Brancaccio, L., Di Crescenzo, G., Rosskopf, C., Santangelo, N., Scarciglia, F., 2000. Carta geologica dei depositi quaternari e carta geomorfologica dell'alta valle del fiume Volturno (Molise, Italia meridionale). Note illustrative. Il Quat. 13, 81–94.

Breda, M., Peretto, C., Thun Hohenstein, U., 2015. The deer from the early Middle Pleistocene site of Isernia la Pineta (Molise, Italy): revised identifications and new remains from the last 15 years of excavation. Geol. J. 50, 290–305.

Britton, K., 2017. A stable relationship: isotopes and bioarchaeology are in it for the long haul. Antiquity 91, 853–864.

Britton, K., Pederzani, S., Kindler, L., Roebroeks, W., Gaudzinski-Windheuser, S., Richards, M.P., Tütken, T., 2019. Oxygen isotope analysis of *Equus* teeth evidences early Eemian and early Weichselian palaeotemperatures at the Middle Palaeolithic site of Neumark-Nord 2, Saxony-Anhalt, Germany. Quat. Sci. Rev. 226, 106029.

Brunetti, M., Maugeri, M., Nanni, T., Simolo, C., Spinoni, J., 2014. High-resolution temperature climatology for Italy: interpolation method intercomparison. Int. J. Climatol. 34, 1278–1296.

Bryant, J.D., Froelich, P.N., 1995. A model of oxygen isotope fractionation in body water of large mammals. Geochem. Cosmochim. Acta 59, 4523–4537.

Buchan, M., Müldner, G., Ervynck, A., Britton, K., 2016. Season of birth and sheep husbandry in late Roman and Medieval coastal Flanders: a pilot study using tooth enamel $\delta^{18}O$ analysis. Environ. Archaeol. 21, 260–270.

Caloi, L., Palombo, M., Zarlenga, F., 1998. Late-Middle Pleistocene mammal faunas of Latium (central Italy): stratigraphy and environment. Quat. Int. 47, 77–86.

Candy, I., Schreve, D.C., Sherriff, J., Tye, G.J., 2014. Marine Isotope Stage 11: Palaeoclimates, palaeoenvironments and its role as an analogue for the current interglacial. Earth Sci. Rev. 128, 18–51.

Carbonell, E., Bermudez de Castro, J.M., Pares, J.M., Perez-Gonzalez, A., Cuenca-Bescos, G., Olle, A., Mosquera, M., Huguet, R., van der Made, J., Rosas, A., Sala, R., Vallverdu, J., Garcia, N., Granger, D.E., Martinon-Torres, M., Rodriguez, X.P., Stock, G.M., Verges, J.M., Allue, E., Burjachs, F., Caceres, I., Canals, A., Benito, A., Diez, C., Lozano, M., Mateos, A., Navazo, M., Rodriguez, J., Rosell, J., Arsuaga, J.L., 2008. The first hominin of Europe. Nature 452, 465–469.

Cavinato, G., Celles, P.D., 1999. Extensional basins in the tectonically bimodal central Apennines fold-thrust belt, Italy: response to corner flow above a subducting slab in retrograde motion. Geology 27, 955–958.

Cerling, T.E., Harris, J.M., 1999. Carbon isotope fractionation between diet and bioapatite in ungulate mammals and implications for ecological and paleoecological studies. Oecologia 120, 347–363.

Channarayapatna, S., Lembo, G., Peretto, C., Thun Hohenstein, U., 2018. Preliminary results from application of GIS to study the distribution of select taphonomic agents and their effects on the faunal remains from 3 colluvium level of Isernia la Pineta. Quaternaire 29 (1), 31–38.

Ciner, B., Wang, Y., Deng, T., Flynn, L., Hou, S., Wu, W., 2015. Stable carbon and oxygen isotopic evidence for Late Cenozoic environmental change in Northern China. Palaeogeogr. Palaeoclimatol. Palaeoecol. 440, 750–762.

Clark, I.D., Fritz, P., 1997. Environmental Isotopes in Hydrogeology. CRC press.

Clauss, M., Polster, C., Kienzle, E., Wiesner, H., Baumgartner, K., von Houwald, F., Streich, W.J., Dierenfeld, E., 2005. Energy and mineral nutrition and water intake in the captive Indian rhinoceros (*Rhinoceros unicornis*). Zoo Biol. 24, 1–14.

Clementz, M.T., 2012. New insight from old bones: stable isotope analysis of fossil mammals. J. Mammal. 93, 368–380.

Collins, R., Jones, M., 1986. The influence of climatic factors on the distribution of C4 species in Europe. Vegetatio 64, 121–129.

Coltorti, M., Cremaschi, M., Delitala, M., Esu, D., Fornaseri, M., McPherron, A., Nicoletti, M., Van Otterloo, R., Peretto, C., Sala, B., 1982. Reversed magnetic polarity at an early Lower Palaeolithic site in Central Italy. Nature 300, 173–176.

Coltorti, M., Feraud, G., Marzoli, A., Peretto, C., Ton-That, T., Voinchet, P., Bahain, J.J., Minelli, A., Thun Hohenstein, U., 2005. New $^{40}Ar/^{39}Ar$, stratigraphic and palaeoclimatic data on the Isernia La Pineta lower Palaeolithic site, Molise, Italy. Quat. Int. 131, 11–22.

Combourieu-Nebout, N., Bertini, A., Russo-Ermolli, E., Peyron, O., Klotz, S., Montade, V., Fauquette, S., Allen, J., Fusco, F., Goring, S., 2015. Climate changes in the central Mediterranean and Italian vegetation dynamics since the Pliocene. Rev. Palaeobot. Palynol. 218, 127–147.

Coplen, T.B., Kendall, C., Hopple, J., 1983. Comparison of stable isotope reference samples. Nature 302, 236–238.

Corrado, S., Di Bucci, D., Naso, G., Butler, R., 1997. Thrusting and strike-slip tectonics in the Alto Molise region (Italy): implications for the Neogene-Quaternary evolution of the Central Apennine orogenic system. J. Geol. Soc. 154, 679–688.

Craig, H., Gordon, L.I., 1965. Deuterium and oxygen 18 variations in the ocean and the marine atmosphere. In: Tongiorgi, E. (Ed.), Stable Isotopes in Oceanographic Studies and Paleotemperatures, pp. 9–130. Spoleto.

Crespi, A., Brunetti, M., Lentini, G., Maugeri, M., 2018. 1961–1990 high-resolution monthly precipitation climatologies for Italy. Int. J. Climatol. 38, 878–895.

Crowley, B.E., Wheatley, P.V., 2014. To bleach or not to bleach? Comparing treatment methods for isolating biogenic carbonate. Chem. Geol. 381, 234–242.

De Castro, J.B., Arsuaga, J.L., Carbonell, E., Rosas, A., Martınez, I., Mosquera, M., 1997. A hominid from the Lower Pleistocene of Atapuerca, Spain: possible ancestor to Neandertals and modern humans. Science 276, 1392–1395.

De Castro, J.M.B., Martinón-Torres, M., Robles, A.G., Prado, L., Carbonell, E., 2010. New human evidence of the Early Pleistocene settlement of Europe, from Sima del Elefante site (Sierra de Atapuerca, Burgos, Spain). Quat. Int. 223, 431–433.

DeNiro, M.J., Epstein, S., 1977. Mechanism of carbon isotope fractionation associated with lipid synthesis. Science 197, 261–263.

DeNiro, M.J., Epstein, S., 1978. Influence of diet on the distribution of carbon isotopes in animals. Geochem. Cosmochim. Acta 42, 495–506.

Dennell, R., Roebroeks, W., 2005. An Asian perspective on early human dispersal from Africa. Nature 438, 1099–1104.
DeSantis, L.R., Wallace, S.C., 2008. Neogene forests from the Appalachians of Tennessee, USA: geochemical evidence from fossil mammal teeth. Palaeogeogr. Palaeoclimatol. Palaeoecol. 266, 59–68.
Desiato, F., Fioravanti, G., Fraschetti, P., Perconti, W., Piervitali, E., 2015. Valori climatici normali di temperatura e precipitazione in Italia. ISPRA. Stato dell'Ambiente 55, 2014.
Desiato, F., Fioravanti, G., Fraschetti, P., Perconti, W., Toreti, A., 2011. Climate indicators for Italy: calculation and dissemination. Adv. Sci. Res. 6, 147–150.
Di Bucci, D., Corrado, S., Naso, G., 2002. Active faults at the boundary between central and southern Apennines (Isernia, Italy). Tectonophysics 359, 47–63.
Di Rita, F., Sottili, G., 2019. Pollen analysis and tephrochronology of a MIS 13 lacustrine succession from eastern Sabatini volcanic district (Rignano Flaminio, central Italy). Quat. Sci. Rev. 204, 78–93.
Dole, M., Lane, G., Rudd, D., Zaukelies, D., 1954. Isotopic composition of atmospheric oxygen and nitrogen. Geochem. Cosmochim. Acta 6, 65–78.
Domingo, L., Koch, P.L., Hernandez Fernandez, M., Fox, D.L., Domingo, M.S., Alberdi, M. T., 2013. Late Neogene and early Quaternary paleoenvironmental and paleoclimatic conditions in southwestern Europe: isotopic analyses on mammalian taxa. PLoS One 8, e63739.
Domínguez-Rodrigo, M., 2014. Is the "savanna hypothesis" a dead concept for explaining the emergence of the earliest hominins? Curr. Anthropol. 55, 59–81.
Driessens, F.C.M., Verbeeck, R.M.H., 1990. Biominerals. CRC Press, Boca Raton, FL.
Drucker, D.G., Bridault, A., Hobson, K.A., Szuma, E., Bocherens, H., 2008. Can carbon-13 in large herbivores reflect the canopy effect in temperate and boreal ecosystems? Evidence from modern and ancient ungulates. Palaeogeogr. Palaeoclimatol. Palaeoecol. 266, 69–82.
Ecker, M., Bocherens, H., Julien, M.A., Rivals, F., Raynal, J.P., Moncel, M.H., 2013. Middle Pleistocene ecology and Neanderthal subsistence: insights from stable isotope analyses in Payre (Ardeche, southeastern France). J. Hum. Evol. 65, 363–373.
Ehleringer, J.R., Monson, R.K., 1993. Evolutionary and ecological aspects of photosynthetic pathway variation. Annu. Rev. Ecol. Systemat. 24, 411–439.
Ermolli, E.R., 1996. Analyse pollinique de la succession lacustre pléistocène du Vallo di Diano (Campanie, Italie). Annales de la Société géologique de Belgique.
Ermolli, E.R., Aucelli, P.P., Di Rollo, A., Mattei, M., Petrosino, P., Porreca, M., Rosskopf, C.M., 2010. An integrated stratigraphical approach to the Middle Pleistocene succession of the Sessano basin (Molise, Italy). Quat. Int. 225, 114–127.
Ermolli, E.R., Brancaccio, L., Santangelo, N., Lirer, L., Juvigne, E., Ozer, A., Bernasconi, S., 1995. The first continental stratotype for four successive isotope stages of the middle Pleistocene for the northern Mediterranean basin: the Vallo di Diano (Campania, Italy). Comptes Rendus de l'Academie des Sciences. Serie 2, Sciences de la Terre et des Planetes 321, 877–884.
Ermolli, E.R., Cheddadi, R., 1997. Climatic reconstruction during the middle Pleistocene: a pollen record from Vallo di Diano (southern Italy). Geobios 30, 735–744.
Ermolli, E.R., Di Donato, V., Martín-Fernández, J.A., Orain, R., Lebreton, V., Piovesan, G., 2015. Vegetation patterns in the Southern Apennines (Italy) during MIS 13: deciphering pollen variability along a NW-SE transect. Rev. Palaeobot. Palynol. 218, 167–183.
Farquhar, G.D., Ehleringer, J.R., Hubick, K.T., 1989. Carbon isotope discrimination and photosynthesis. Annu. Rev. Plant Biol. 40, 503–537.
Feranec, R.S., Hadly, E.A., Paytan, A., 2009. Stable isotopes reveal seasonal competition for resources between late Pleistocene bison (*Bison*) and horse (*Equus*) from Rancho La Brea, southern California. Palaeogeogr. Palaeoclimatol. Palaeoecol. 271, 153–160.
Fernandes, C.A., Rohling, E.J., Siddall, M., 2006. Absence of post-Miocene Red Sea land bridges: biogeographic implications. J. Biogeogr. 33, 961–966.
Flanagan, L.B., Bain, J.F., Ehleringer, J.R., 1991. Stable oxygen and hydrogen isotope composition of leaf water in C_3 and C_4 plant species under field conditions. Oecologia 88, 394–400.
Fortelius, M., Mazza, P., Sala, B., 1993. *Stephanorhinus* (Mammalia: Rhinocerotidae) of the western European Pleistocene, with a revision of *S. etruscus* (Falconer, 1868). Palaeontogr. Ital. 80, 63–155.
Fricke, H., 2010. Stable Isotope Geochemistry of Bonebed Fossils: Reconstructing Paleoenvironments, Paleoecology, and Paleobiology. Bonebeds. University of Chicago Press, pp. 437–490.
Gabunia, L., Vekua, A., Lordkipanidze, D., Swisher, C.C., Ferring, R., Justus, A., Nioradze, M., Tvalchrelidze, M., Antón, S.C., Bosinski, G., 2000. Earliest Pleistocene hominid cranial remains from Dmanisi, Republic of Georgia: taxonomy, geological setting, and age. Science 288, 1019–1025.
Gadbury, C., Todd, L., Jahren, A.H., Amundson, R., 2000. Spatial and temporal variations in the isotopic composition of bison tooth enamel from the early Holocene Hudson-Meng Bone Bed, Nebraska. Palaeogeography, Palaeoclimatogy, Palaeoecoogy 157, 79–93.
Gallotti, R., Peretto, C., 2015. The lower/early middle Pleistocene small débitage productions in western Europe: new data from Isernia La Pineta t. 3c (upper Volturno basin, Italy). Quat. Int. 357, 264–281.
Giusberti, G., Peretto, C., 1991. Evidences de la fracturation intentionnelle d'ossements animaux avec moelle dans le gisement de «La Pineta» de Isernia (Molise), Italie. L'Anthropologie 85, 765–778.
Giustini, F., Brilli, M., Patera, A., 2016. Mapping oxygen stable isotopes of precipitation in Italy. J. Hydrol.: Reg. Stud. 8, 162–181.
Green, D.R., Green, G.M., Colman, A.S., Bidlack, F.B., Tafforeau, P., Smith, T.M., 2017. Synchrotron imaging and Markov chain Monte Carlo reveal tooth mineralization patterns. PLoS One 12, e0186391.
Groves, C.P., 1967. On the rhinoceroses of south-east Asia. Säugetierkundliche Mitteilungen 15, 221–237.
Guérin, C., 1980. In: Les rhinoceros (Mammalia, Perissodactyla) du Miocene terminal au Pleistocene superieur en Europe occidentale: comparison avec les especes actuelles, vol. 79. Documents du Laboratoire de Géologie de la Faculté des Sciences de Lyon, pp. 1–1182.
Harris, E.B., Kohn, M.J., Strömberg, C.A., 2020. Stable isotope compositions of herbivore teeth indicate climatic stability leading into the mid-Miocene Climatic Optimum. In: Idaho (Ed.), USA. Palaeogeography, Palaeoclimatology, Palaeoecology, vol. 546, p. 109610.
Hartman, G., Danin, A., 2010. Isotopic values of plants in relation to water availability in the Eastern Mediterranean region. Oecologia 162, 837–852.
Heaton, T.H.E., 1999. Spatial, species, and temporal variations in the $^{13}C/^{12}C$ ratios of C_3 plants: implications for paleodiet studies. J. Archaeol. Sci. 26, 637–649.
Hernesniemi, E., Blomstedt, K., Fortelius, M., 2011. Multi-view stereo three-dimensional reconstruction of lower molars of recent and Pleistocene rhinoceroses for mesowear analysis. Palaeontol. Electron. 14, 1–15.
Holmes, K.M., 2007. Using Pliocene palaeoclimatic data to postulate dispersal pathways of early hominins. Palaeogeogr. Palaeoclimatol. Palaeoecol. 248, 96–108.
Hoppe, K.A., Amundson, R., Vavra, M., McClaran, M.P., Anderson, D.L., 2004a. Isotopic analysis of tooth enamel carbonate from modern North American feral horses: implications for paleoenvironmental reconstructions. Palaeogeography, Palaeoclimatogy, Palaeoecoogy 203, 299–311.
Hoppe, K.A., Stover, S.M., Pascoe, J.R., Amundson, R., 2004b. Tooth enamel biomineralization in extant horses: implications for isotopic microsampling. Palaeogeography, Palaeoclimatogy, Palaeoecoogy 206, 355–365.
Hoppe, K.A., Stuska, S., Amundson, R., 2005. The implications for paleodietary and paleoclimatic reconstructions of intrapopulation variability in the oxygen and carbon isotopes of teeth from modern feral horses. Quat. Res. 64, 138–146.
Hublin, J.-J., 2009. The origin of Neandertals. Proc. Natl. Acad. Sci. Unit. States Am. 106, 16022–16027.
Julien, M.-A., Bocherens, H., Burke, A., Drucker, D.G., Patou-Mathis, M., Krotova, O., Péan, S., 2012. Were European steppe bison migratory? ^{18}O, ^{13}C and Sr intra-tooth isotopic variations applied to a palaeoethological reconstruction. Quat. Int. 271, 106–119.
Kahlke, R.-D., García, N., Kostopoulos, D.S., Lacombat, F., Lister, A.M., Mazza, P.P.A., Spassov, N., Titov, V.V., 2011. Western Palaearctic palaeoenvironmental conditions during the Early and early Middle Pleistocene inferred from large mammal communities, and implications for hominin dispersal in Europe. Quat. Sci. Rev. 30, 1368–1395.
Kahlke, R.-D., Kaiser, T.M., 2011. Generalism as a subsistence strategy: advantages and limitations of the highly flexible feeding traits of Pleistocene *Stephanorhinus hundsheimensi* (Rhinocerotidae, Mammalia). Quat. Sci. Rev. 30, 2250–2261.
Karner, D., Juvigne, E., Brancaccio, L., Cinque, A., Ermolli, E.R., Santangelo, N., Bernasconi, S., Lirer, L., 1999. A potential early middle Pleistocene tephrostratotype for the Mediterranean basin: the Vallo di Diano, Campania, Italy. Global Planet. Change 21, 1–15.
Kingston, J.D., 2007. Shifting adaptive landscapes: progress and challenges in reconstructing early hominid environments. Am. J. Phys. Anthropol. 134, 20–58.
Koch, P.L., 1998. Isotopic reconstruction of past continental environments. Annual Review Earth and Planetary Science Letters 26, 573–613.
Koch, P.L., Michener, R., Lajtha, K., 2007. Isotopic study of the biology of modern and fossil vertebrates. Stable Isotopes in Ecology and Environmental Science 2, 99–154.
Koch, P.L., Tuross, N., Fogel, M.L., 1997. The effects of sample treatment and diagenesis on the isotopic integrity of carbonate in biogenic hydroxylapatite. J. Archaeol. Sci. 24, 417–429.
Kohn, M.J., 1996. Predicting animal $\delta^{18}O$: accounting for diet and physiological adaptation. Geochem. Cosmochim. Acta 60, 4811–4829.
Kohn, M.J., 2010. Carbon isotope composition of terrestrial C3 plants as indicators of (paleo)ecology and (paleo)climate. Proc. Natl. Acad. Sci. Unit. States Am. 107, 19691–19695.
Kohn, M.J., 2016. Carbon isotope discrimination in C3 land plants is independent of natural variations in p_{CO2}. Geochemical Perspectives Letters 35–43.
Kohn, M.J., Cerling, T.E., 2002. Stable isotope compositions of biological apatite. Rev. Mineral. Geochem. 48, 455–488.
Kohn, M.J., Fremdt, T.J., 2007. Tectonic controls on isotope compositions and species diversification. John Day Basin, central Oregon. Paleobios 27, 48–61.
Kohn, M.J., McKay, M.P., 2012. Paleoecology of late Pleistocene–Holocene faunas of eastern and central Wyoming, USA, with implications for LGM climate models. Palaeogeogr. Palaeoclimatol. Palaeoecol. 326–328, 42–53.
Kohn, M.J., McKay, M.P., Knight, J.L., 2005. Dining in the Pleistocene-who's on the menu? Geology 33, 649–652.
Kohn, M.J., Schoeninger, M.J., Barker, W.W., 1999. Altered states: effects of diagenesis on fossil tooth chemistry. Geochem. Cosmochim. Acta 18, 2737–2747.
Kohn, M.J., Schoeninger, M.J., Valley, J.W., 1996. Herbivore tooth oxygen isotope compositions: effect of diet and physiology. Geochem. Cosmochim. Acta 60, 3889–3896.
Kroll, E.M., 1994. Behavioral implications of Plio-Pleistocene archaeological site structure. J. Hum. Evol. 27, 107–138.
Kroopnick, P., Craig, H., 1972. Atmospheric oxygen: isotopic composition and solubility fractionation. Science 175, 54–55.
Lacombat, F., 2005. Les rhinocéros fossiles des sites préhistoriques de l'Europe méditerranéenne et du Massif Central. Paléontologie et implications bio-chronologiques. BAR Int. Ser. 1419.
Lacombat, F., 2006. Pleistocene rhinoceroses in Mediterranean Europe and in Massif central (France). Cour. Forschungsinst. Senckenberg 256, 57.

Lebreton, V., 2002. Végétation et climat au Pléistocène inférieur et moyen à La Pineta (Isernia, Italie). Comptes Rendus Palevol 1, 11–17.
Leroy, S.A.G., Arpe, K., Mikolajewicz, U., 2011. Vegetation context and climatic limits of the Early Pleistocene hominin dispersal in Europe. Quat. Sci. Rev. 30, 1448–1463.
Levin, N.E., 2015. Environment and climate of early human evolution. Annu. Rev. Earth Planet Sci. 43, 405–429.
Levin, N.E., Cerling, T.E., Passey, B.H., Harris, J.M., Ehleringer, J.R., 2006. A stable isotope aridity index for terrestrial environments. Proc. Natl. Acad. Sci. U.S.A. 103, 11201–11205.
Lisiecki, L.E., Raymo, M.E., 2005. A Pliocene-Pleistocene stack of 57 globally distributed benthic $\delta^{18}O$ records. Paleoceanography 20.
Longinelli, A., 1984. Oxygen isotopes in mammal bone phosphate: a new tool for paleohydrological and paleoclimatological research? Geochem. Cosmochim. Acta 48, 385–390.
Longinelli, A., Selmo, E., 2003. Isotopic composition of precipitation in Italy: a first overall map. J. Hydrol. 270, 75–88.
López-García, J.M., Berto, C., Luzi, E., Dalla Valle, C., Bañuls-Cardona, S., Sala, B., 2015a. The genus *Iberomys* (Rodentia, Arvicolinae, Mammalia) in the Pleistocene of Italy. Italian Journal of Geosciences 134, 162–169.
López-García, J.M., Luzi, E., Berto, C., Peretto, C., Arzarello, M., 2015b. Chronological context of the first hominin occurrence in southern Europe: the *Allophaiomys ruffoi* (Arvicolinae, Rodentia, Mammalia) from Pirro 13 (Pirro Nord, Apulia, southwestern Italy). Quat. Sci. Rev. 107, 260–266.
Lorenzo, C., Pablos, A., Carretero, J.M., Huguet, R., Valverdú, J., Martinón-Torres, M., Arsuaga, J.L., Carbonell, E., de Castro, J.M.B., 2015. Early Pleistocene human hand phalanx from the Sima del Elefante (TE) cave site in Sierra de Atapuerca (Spain). J. Hum. Evol. 78, 114–121.
Lugli, F., Cipriani, A., Peretto, C., Mazzucchelli, M., Brunelli, D., 2017. In situ high spatial resolution $^{87}Sr/^{86}Sr$ ratio determination of two Middle Pleistocene (ca 580 ka) Stephanorhinus hundsheimensis teeth by LA–MC–ICP–MS. Int. J. Mass Spectrom. 412, 38–48.
Luyt, J., Sealy, J., 2018. Inter-tooth comparison of $\delta^{13}C$ and $\delta^{18}O$ in ungulate tooth enamel from south-western Africa. Quat. Int. 495, 144–152.
Luz, B., Kolodny, Y., Horowitz, M., 1984. Fractionation of oxygen isotopes between mammalian bone-phosphate and environmental drinking water. Geochem. Cosmochim. Acta 48, 1689–1693.
Macdonald, D.W., 2007. The Encyclopedia of Mammals. Oxford University Press.
MacFadden, B.J., Higgins, P., 2004. Ancient ecology of 15-million-years-old browsing mammals within C_3 plant communities from Panama. Oecologia 140, 169–182.
Manzi, G., Magri, D., Palombo, M.R., 2011. Early–Middle Pleistocene environmental changes and human evolution in the Italian peninsula. Quat. Sci. Rev. 30, 1420–1438.
Marcolini, F., Zanchetta, G., Bonadonna, F., 2001. Some preliminary data on two small mammal bearing paleosols from the Tyrrhenian and Adriatic sides of Italy. Oryctos 3, 85–94.
Martin, C., Bentaleb, I., Kaandorp, R., Iacumin, P., Chatri, K., 2008. Intra-tooth study of modern rhinoceros enamel $\delta^{18}O$: is the difference between phosphate and carbonate $\delta^{18}O$ a sound diagenetic test? Palaeogeogr. Palaeoclimatol. Palaeoecol. 266, 183–189.
Matson, S.D., Rook, L., Oms, O., Fox, D.L., 2012. Carbon isotopic record of terrestrial ecosystems spanning the Late Miocene extinction of Oreopithecus bambolii, Baccinello Basin (Tuscany, Italy). J. Hum. Evol. 63, 127–139.
Mazza, P., Azzaroli, A., 1993. Ethological inferences on Pleistocene rhinoceroses of Europe. Rendiconti Lincei 4, 127.
Mazza, P., Sala, B., Fortelius, M., 1993. A small latest Villafranchian (late early Pleistocene) rhinoceros from Pietrafitta (Perugia, Umbria, Central Italy), with notes on the Pirro and Westerhoven rhinoceroses. Palaeontogr. Ital. 80, 25–50.
Messager, E., Lebreton, V., Marquer, L., Russo-Ermolli, E., Orain, R., Renault-Miskovsky, J., Lordkipanidze, D., Despriée, J., Peretto, C., Arzarello, M., 2011. Palaeoenvironments of early hominins in temperate and Mediterranean Eurasia: new palaeobotanical data from Palaeolithic key-sites and synchronous natural sequences. Quat. Sci. Rev. 30, 1439–1447.
Moncel, M.-H., 2010. Oldest human expansions in Eurasia: favouring and limiting factors. Quat. Int. 223, 1–9.
Moncel, M.-H., Ashton, N., Arzarello, M., Fontana, F., Lamotte, A., Scott, B., Muttillo, B., Berruti, G., Nenzioni, G., Tuffreau, A., 2020. Early Levallois core technology between marine isotope stage 12 and 9 in Western Europe. J. Hum. Evol. 139, 102735.
Montuire, S., Marcolini, F., 2002. Palaeoenvironmental significance of the mammalian faunas of Italy since the Pliocene. J. Quat. Sci. 17, 87–96.
Moyano, I.T., Barsky, D., Cauche, D., Celiberti, V., Grégoire, S., Lebegue, F., Moncel, M. H., De Lumley, H., 2011. The archaic stone tool industry from Barranco León and Fuente Nueva 3 (Orce, Spain): evidence of the earliest hominin presence in southern Europe. Quat. Int. 243, 80–91.
Murphy, B.P., Bowman, D.M., Gagan, M.K., 2007. The interactive effect of temperature and humidity on the oxygen isotope composition of kangaroos. Funct. Ecol. 21, 757–766.
Muttoni, G., Scardia, G., Kent, D.V., 2010. Human migration into Europe during the late Early Pleistocene climate transition. Palaeogeogr. Palaeoclimatol. Palaeoecol. 296, 79–93.
Muttoni, G., Scardia, G., Kent, D.V., Morsiani, E., Tremolada, F., Cremaschi, M., Peretto, C., 2011. First dated human occupation of Italy at ~ 0.85 Ma during the late Early Pleistocene climate transition. Earth Planet Sci. Lett. 307, 241–252.
O'Leary, 1988. Carbon isotopes in photosynthesis. Bioscience 38, 328–336.
Orain, R., Lebreton, V., Ermolli, E.R., Combourieu-Nebout, N., Sémah, A.-M., 2013a. *Carya* as marker for tree refuges in southern Italy (Boiano basin) at the Middle Pleistocene. Palaeogeogr. Palaeoclimatol. Palaeoecol. 369, 295–302.
Orain, R., Lebreton, V., Russo Ermolli, E., Aucelli, P., Amato, V., 2012. Végétation et climat au Pléistocène moyen en Italie méridionale (Bassin de Boiano, Molise). Quaternaire 23, 37–48.
Orain, R., Lebreton, V., Russo Ermolli, E., Sémah, A.-M., Nomade, S., Shao, Q., Bahain, J.-J., Thun Hohenstein, U., Peretto, C., 2013b. Hominin responses to environmental changes during the Middle Pleistocene in central and southern Italy. Clim. Past 9, 687–697.
Osthoff, G., Beukes, B., Steyn, A.C., Hugo, A., Deacon, F., Butler, H.J., O'Neill, F.H., Grobler, J.P., 2021. Milk composition of white rhinoceros over lactation and comparison with other Perissodactyla. Zoo Biol. 40, 417–428.
Owen, R.B., Muiruri, V.M., Lowenstein, T.K., Renaut, R.W., Rabideaux, N., Luo, S., Deino, A.L., Sier, M.J., Dupont-Nivet, G., McNulty, E.P., 2018. Progressive aridification in East Africa over the last half million years and implications for human evolution. Proc. Natl. Acad. Sci. Unit. States Am. 115, 11174–11179.
Palombo, M.R., Sardella, R., 2007. Biochronology and biochron boundaries: a real dilemma or a false problem? An example based on the Pleistocene large mammalian faunas from Italy. Quat. Int. 160, 30–42.
Pandolfi, L., Fiore, I., Gaeta, M., Szabó, P., Vennemann, T., Tagliacozzo, A., 2018. Rhinocerotidae (Mammalia, Perissodactyla) from the middle Pleistocene levels of Grotta Romanelli (Lecce, southern Italy). Geobios 51, 453–468.
Passey, B.H., Cerling, T.E., 2002. Tooth enamel mineralization in ungulates: implications for recovering a primary isotopic time-series. Geochem. Cosmochim. Acta 66, 3225–3234.
Passey, B.H., Robinson, T.F., Ayliffe, L.K., Cerling, T.E., Sponheimer, M., Dearing, M.D., Roeder, B.L., Ehleringer, J.R., 2005. Carbon isotope fractionation between diet, breath CO_2, and bioapatite in different mammals. J. Archaeol. Sci. 32, 1459–1470.
Patterson, D., Braun, D., Behrensmeyer, A.K., Lehmann, S., Merritt, S., Reeves, J., Wood, B., Bobe, R., 2017. Landscape scale heterogeneity in the east Turkana ecosystem during the Okote Member (1.56–1.38 Ma). J. Hum. Evol. 112, 148–161.
Pederzani, S., Britton, K., 2019. Oxygen isotopes in bioarchaeology: principles and applications, challenges and opportunities. Earth Sci. Rev. 188, 77–107.
Pereira, A., Nomade, S., Shao, Q., Bahain, J.-J., Arzarello, M., Douville, E., Falgueres, C., Frank, N., Garcia, T., Lembo, G., 2016. $^{40}Ar/^{39}Ar$ and ESR/U-series dates for Guado san Nicola, middle Pleistocene key site at the lower/middle Palaeolithic transition in Italy. Quat. Geochronol. 36, 67–75.
Pereira, A., Nomade, S., Voinchet, P., Bahain, J.J., Falguères, C., Garon, H., Lefèvre, D., Raynal, J.P., Scao, V., Piperno, M., 2015. The earliest securely dated hominin fossil in Italy and evidence of Acheulian occupation during glacial MIS 16 at Notarchirico (Venosa, Basilicata, Italy). J. Quat. Sci. 30, 639–650.
Peretto, C., 2006. The first peopling of southern Europe: the Italian case. Comptes Rendus Palevol 5, 283–290.
Peretto, C., Amore, F.O., Antoniazzi, A., Antoniazzi, A., Bahain, J.-J., Cattani, L., Cavallini, E., Esposito, P., Falguères, C., Gagnepain, J., 1998. L'industrie lithique de Ca' Belvedere di Monte Poggiolo: stratigraphie, matiere premiere, typologie, remontages et traces d'utilisation. L'Anthropologie 102, 343–465.
Peretto, C., Arnaud, J., Moggi-Cecchi, J., Manzi, G., Nomade, S., Pereira, A., Falgueres, C., Bahain, J.J., Grimaud-Herve, D., Berto, C., Sala, B., Lembo, G., Muttillo, B., Gallotti, R., Thun Hohenstein, U., Vaccaro, C., Coltorti, M., Arzarello, M., 2015a. A human deciduous tooth and new $^{40}Ar/^{39}Ar$ dating results from the middle Pleistocene archaeological site of Isernia La Pineta, southern Italy. PLoS One 10, e0140091.
Peretto, C., Arzarello, M., Bahain, J.-J., Boulbes, N., Dolo, J.-M., Douville, E., Falguères, C., Frank, N., Garcia, T., Lembo, G., Moigne, A.-M., Muttillo, B., Nomade, S., Pereira, A., Rufo, M.A., Sala, B., Shao, Q., Thun Hohenstein, U., Tessari, U., Turrini, M.C., Vaccaro, C., 2015b. The middle Pleistocene site of Guado san Nicola (Monteroduni, Central Italy) on the lower/middle Palaeolithic transition. Quat. Int. 411, 301–315.
Peretto, C., Biagi, P., Boschian, G., Broglio, A., De Stefani, M., Fasani, L., Fontana, F., Grifoni, R., Guerreschi, A., Iacopini, A., Minelli, A., Pala, R., Peresani, M., Radi, G., Ronchitelli, A., Sarti, L., Thun Hohenstein, U., Tozzi, C., 2004. Living-floors and structures from the Lower Palaeolithic to the Bronze Age in Italy. Coll. Antropol. 28 (1), 63–88.
Petrella, E., Capuano, P., Carcione, M., Celico, F., 2009. A high-altitude temporary spring in a compartmentalized carbonate aquifer: the role of low-permeability faults and karst conduits. Hydrol. Process. 23, 3354–3364.
Petrella, E., Celico, F., 2013. Mixing of water in a carbonate aquifer, southern Italy, analysed through stable isotope investigations. Int. J. Speleol. 42, 4.
Picin, A., Peresani, M., Falguères, C., Gruppioni, G., Bahain, J.-J., 2013. San Bernardino Cave (Italy) and the appearance of Levallois technology in Europe: results of a radiometric and technological reassessment. PLoS One 8, e76182.
Potts, R., 2013. Hominin evolution in settings of strong environmental variability. Quat. Sci. Rev. 73, 1–13.
Potts, R., Behrensmeyer, A.K., Faith, J.T., Tryon, C.A., Brooks, A.S., Yellen, J.E., Deino, A. L., Kinyanjui, R., Clark, J.B., Haradon, C.M., 2018. Environmental dynamics during the onset of the middle stone age in eastern Africa. Science 360, 86–90.
Potts, R., Dommain, R., Moerman, J.W., Behrensmeyer, A.K., Deino, A.L., Riedl, S., Beverly, E.J., Brown, E.T., Deocampo, D., Kinyanjui, R., 2020. Increased ecological resource variability during a critical transition in hominin evolution. Sci. Adv. 6.
Potts, R., Faith, J.T., 2015. Alternating high and low climate variability: the context of natural selection and speciation in Plio-Pleistocene hominin evolution. J. Hum. Evol. 87, 5–20.
Pryor, A.J.E., Stevens, R.E., O'Connell, T.C., Lister, J.R., 2014. Quantification and propagation of errors when converting vertebrate biomineral oxygen isotope data to

temperature for palaeoclimate reconstruction. Palaeogeogr. Palaeoclimatol. Palaeoecol. 412, 99–107.
Radmilli, A.M., Boschian, G., 1996. Gli scavi a Castel di Guido: il più antico giacimento di cacciatori del Paleolitico inferiore nell'Agro Romano. Istituto italiano di preistoria e protostoria.
Roebroeks, W., Van Kolfschoten, T., 1994. The earliest occupation of Europe: a short chronology. Antiquity 68, 489–503.
Rozanski, K., Araguas-Araguas, L., Gonfiantini, R., 1993. Isotopic paterns in modern global precipitation. In: Climate Change in Continental Isotopic Records. American Geophysical Union, Washington DC, pp. 1–36.
Saarinen, J., Eronen, J., Fortelius, M., Seppä, H., Lister, A.M., 2016. Patterns of diet and body mass of large ungulates from the Pleistocene of Western Europe, and their relation to vegetation. Palaeontol. Electron. 19, 1–58.
Saarinen, J., Oksanen, O., Žliobaitė, I., Fortelius, M., DeMiguel, D., Azanza, B., Bocherens, H., Luzón, C., Solano-García, J., Yravedra, J., 2021. Pliocene to Middle Pleistocene climate history in the Guadix-Baza Basin, and the environmental conditions of early Homo dispersal in Europe. Quat. Sci. Rev. 268, 107132.
Sala, B., 1983. La fauna del giacimento di Isernia La Pineta (nota preliminare). In: Isernia La Pineta: Un Accampamento Piu' Antico di 700000 Anni, Catalogo della Mostra. Calderini, Bologna, pp. 71–79.
Sala, B., 1996. Gli animali del giacimento di Isernia La Pineta. In: Peretto, C. (Ed.), I Reperti Paleontologici del Giacimento Paleolitico di Isernia La Pineta, l'Uomo e l'Ambiente. Cosmo Iannone Editore, Isernia, pp. 25–49.
Sala, B., 2006. Le nuove specie rinvenute a La Pineta. In: Peretto, C., Minelli, A. (Eds.), Preistoria in Molise, Gli Insediamenti del Territorio di Isernia. Centro Europeo di Ricerche Preistoriche, Collana Ricerche. Aracne Editrice, Isernia, pp. 36–38.
Sardella, R., Palombo, M.R., Petronio, C., Bedetti, C., Pavia, M., 2006. The early Middle Pleistocene large mammal faunas of Italy: an overview. Quat. Int. 149, 104–109.
Schreiber, H.D., 2005. Osteological investigations on skeleton material of rhinoceroses (Rhinocerotidae, Mammalia) from the early Middle Pleistocene locality of Mauer near Heidelberg (SW-Germany). Quaternaire 2, 103–111.
Siepielski, A.M., Morrissey, M.B., Buoro, M., Carlson, S.M., Caruso, C.M., Clegg, S.M., Coulson, T., DiBattista, J., Gotanda, K.M., Francis, C.D., 2017. Precipitation drives global variation in natural selection. Science 355, 959–962.
Skrzypek, G., Sadler, R., Wiśniewski, A., 2016. Reassessment of recommendations for processing mammal phosphate $\delta^{18}O$ data for paleotemperature reconstruction. Palaeogeogr. Palaeoclimatol. Palaeoecol. 446, 162–167.
Steudel, K.L., 1994. Locomotor energetics and hominid evolution. Evol. Anthropol. 3, 42–48.
Suga, S., 1982. Progressive mineralization pattern of developing enamel during the maturation stage. J. Dent. Res. 1532–1542.
Tafforeau, P., Bentaleb, I., Jaeger, J.-J., Martin, C., 2007. Nature of laminations and mineralization in rhinoceros enamel using histology and X-ray synchrotron microtomography: potential implications for palaeoenvironmental isotopic studies. Palaeogeogr. Palaeoclimatol. Palaeoecol. 246, 206–227.
Tejada-Lara, J.V., MacFadden, B.J., Bermudez, L., Rojas, G., Salas-Gismondi, R., Flynn, J. J., 2018. Body mass predicts isotope enrichment in herbivorous mammals. Proceedings of the Royal Society B 285, 20181020.
Thun Hohenstein, U., Di Nucci, A., Moigne, A.-M., 2009. Mode de vie à Isernia La Pineta (Molise, Italie). Stratégie d'exploitation du Bison schoetensacki par les groupes humains au Paléolithique inférieur. L'anthropologie 113, 96–110.
Thun Hohenstein, U., Malerba, G., Ghirelli, E., Giacobini, G., Peretto, C., 2002. Attività di sussistenza nel Paleolitico inferiore di Isernia La Pineta: archeozoologia delle US3S10 e 3 coll (scavi 2000). Rivista di Scienze Preistoriche 3–20.
Thun Hohenstein, U., Malerba, G., Giacobini, G., Peretto, C., 2004. Bone surface micromorphological study of the faunal remains from the Lower Palaeolithic site of Isernia La Pineta (Molise, Italy), XIV Congres de l'Union Internationale des Sciences Prehistoriques et Protohistoriques. Archaeopress 123–129.
Tipple, B.J., Meyers, S.R., Pagani, M., 2010. Carbon isotope ratio of Cenozoic CO_2: a comparative evaluation of available geochemical proxies. Paleoceanography 25.
Tong, H., 2001. Age profiles of rhino fauna from the Middle Pleistocene Nanjing man site, south China—explained by the rhino specimens of living species. Int. J. Osteoarchaeol. 11, 231–237.
Tonon, M., 1988. Note sull'avifauna del deposito di Isernia La Pineta. Il Quat. 2, 171–173.
Toro-Moyano, I., De Lumley, H., Fajardo, B., Barsky, D., Cauche, D., Celiberti, V., Grégoire, S., Martinez-Navarro, B., Espigares, M.P., Ros-Montoya, S., 2009. L'industrie lithique des gisements du Pléistocène inférieur de Barranco León et Fuente Nueva3 à Orce, Grenade, Espagne. L'Anthropologie 113, 111–124.
Trayler, R.B., Kohn, M.J., 2017. Tooth enamel maturation reequilibrates oxygen isotope compositions and supports simple sampling methods. Geochem. Cosmochim. Acta 198, 32–47.
Tütken, T., Vennemann, T.W., Janz, H., Heizmann, E.P.J., 2006. Palaeoenvironment and palaeoclimate of the Middle Miocene lake in the Steinheim basin, SW Germany: a reconstruction from C, O, and Sr isotopes of fossil remains. Palaeogeogr. Palaeoclimatol. Palaeoecol. 241, 457–491.
Urban, M.A., Nelson, D.M., Jiménez-Moreno, G., Hu, F.S., 2016. Carbon isotope analyses reveal relatively high abundance of C_4 grasses during early–middle Miocene in southwestern Europe. Palaeogeogr. Palaeoclimatol. Palaeoecol. 443, 10–17.
van Asperen, E.N., Kahlke, R.-D., 2015. Dietary variation and overlap in Central and Northwest European *Stephanorhinus kirchbergensiss* and *S. hemitoechus* (Rhinocerotidae, Mammalia) influenced by habitat diversity. Quat. Sci. Rev. 107, 47–61.
van der Made, J., 2005. Considerations on dispersals between Africa and Europe across the Strait of Gibraltar. In: Cuaternario Mediterraneo y poblamiento de hominidos. AEQUA & Gibraltar Museum, Gibraltar, pp. 91–92.
van der Made, J., 2010. The rhinos from the middle Pleistocene of Neumark-Nord (Saxony-Anhalt). Veröffentlichungen des Landesamtes für Archeologie 62, 432–527.
van der Made, J., Mateos, A., 2010. Longstanding biogeographic patterns and the dispersal of early *Homo* out of Africa and into Europe. Quat. Int. 223–224, 195–200.
van der Merwe, N.J., Medina, E., 1991. The canopy effect, carbon isotope ratios and foodwebs in Amazonia. J. Archaeol. Sci. 18, 249–259.
Villa, P., 2001. Early Italy and the colonization of western Europe. Quat. Int. 75, 113–130.
Villa, V., Pereira, A., Chaussé, C., Nomade, S., Giaccio, B., Limondin-Lozouet, N., Fusco, F., Regattieri, E., Degeai, J.-P., Robert, V., 2016. A MIS 15-MIS 12 record of environmental changes and Lower Palaeolithic occupation from Valle Giumentina, central Italy. Quat. Sci. Rev. 151, 160–184.
Walker, A., Leakey, R.E., Leakey, R., 1993. The Nariokotome Homo Erectus Skeleton. Harvard University Press.
Zanazzi, A., Judd, E., Fletcher, A., Bryant, H., Kohn, M.J., 2015. Eocene–Oligocene latitudinal climate gradients in North America inferred from stable isotope ratios in perissodactyl tooth enamel. Palaeogeogr. Palaeoclimatol. Palaeoecol. 417, 561–568.
Zanazzi, A., Kohn, M.J., 2008. Ecology and physiology of White River mammals based on stable isotope ratios of teeth. Palaeogeogr. Palaeoclimatol. Palaeoecol. 257, 22–37.
Zazzo, A., Balasse, M., Patterson, W.P., 2005. High-resolution $\delta^{13}C$ intratooth profiles in bovine enamel: implications for mineralization pattern and isotopic attenuation. Geochem. Cosmochim. Acta 69, 3631–3642.
Zazzo, A., Lecuyer, C., Mariotti, A., 2004. Experimentally-controlled carbon and oxygen isotope exchange between bioapatites and water under inorganic and microbially-mediated conditions. Geochem. Cosmochim. Acta 68, 1–12.
Zazzo, A., Mariotti, A., Lecuyer, C., Heintz, E., 2002. Intra-tooth isotope variations in late Miocene bovid enamel from Afghanistan: paleobiological, taphonomic, and climatic implications. Palaeogeography, Palaeoclimatogy, Palaeoecoogy 186, 145–161.
Zhang, C., Wang, Y., Li, Q., Wang, X., Deng, T., Tseng, Z.J., Takeuchi, G.T., Xie, G., Xu, Y., 2012. Diets and environments of late cenozoic mammals in the Qaidam basin, Tibetan plateau: evidence from stable isotopes. Earth Planet Sci. Lett. 333, 70–82.
Zin Maung Maung, T., Takai, M., Uno, H., Wynn, J.G., Egi, N., Tsubamoto, T., Thaung, H., Aung Naing, S., Maung, M., Nishimura, T., Yoneda, M., 2011. Stable isotope analysis of the tooth enamel of Chaingzauk mammalian fauna (late Neogene, Myanmar) and its implication to paleoenvironment and paleogeography. Palaeogeogr. Palaeoclimatol. Palaeoecol. 300, 11–22.